

Hydro-mechanical evolution of the EDZ as transport path for radionuclides and gas: insights from the Mont Terri rock laboratory (Switzerland)

Paul Marschall¹ · Silvio Giger¹ · Rémi De La Vassière² · Hua Shao³ ·
Helen Leung⁴ · Christophe Nussbaum⁵ · Thomas Trick⁶ · Bill Lanyon⁷ ·
Rainer Senger⁸ · Andrea Lisjak⁹ · Andrés Alcolea¹⁰

Received: 29 March 2016 / Accepted: 9 December 2016 / Published online: 17 February 2017
© Swiss Geological Society 2017

Abstract The excavation damaged zone (EDZ) around the backfilled underground structures of a geological repository represents a release path for radionuclides, which needs to be addressed in the assessment of long-term safety. Additionally, the EDZ may form a highly efficient escape route for corrosion and degradation gases, thus limiting the gas overpressures in the backfilled repository structures. The efficiency of this release path depends not only on the shape and extent of the EDZ, but also on the self-sealing capacity of the host rock formation and the prevailing state conditions, such as in situ stresses and pore pressure. The hydro-mechanical and chemico-osmotic phenomena associated with the formation and temporal evolution of the EDZ are complex, thus precluding a detailed representation of the EDZ in conventional

modelling tools for safety assessment. Therefore, simplified EDZ models, able to mimic the safety-relevant functional features of the EDZ in a traceable manner are required. In the framework of the Mont Terri Project, a versatile modelling approach has been developed for the simulation of flow and transport processes along the EDZ with the goal of capturing the evolution of hydraulic significance of the EDZ after closure of the backfilled underground structures. The approach draws on both empirical evidence and experimental data, collected in the niches and tunnels of the Mont Terri rock laboratory. The model was benchmarked with a data set from an in situ self-sealing experiment at the Mont Terri rock laboratory. This paper summarises the outcomes of the benchmark exercise that comprises relevant empirical evidence, experimental data bases and the conceptual framework for modelling the evolution of the hydraulic significance of the EDZ around a backfilled tunnel section during the entire re-saturation phase.

Editorial handling: P. Bossart and A. G. Milnes.

The abbreviations EDB, EZ-A, EZ-B, FE, GP, GP-A, GS, HG-A, SE-H denote in situ experiments at the Mont Terri rock laboratory.

This is paper #8 of the Mont Terri Special Issue of the Swiss Journal of Geosciences (see Bossart et al. 2017, Table 3 and Fig. 7).

✉ Paul Marschall
paul.marschall@nagra.ch

¹ National Cooperative for the Disposal of Radioactive Waste NAGRA, Hardstrasse 73, 5430 Wettingen, Switzerland

² Agence Nationale pour la Gestion des Déchets Radioactifs ANDRA, Meuse Haute-Marne, Center RD 960, 55500 Bure, France

³ Federal Institute for Geosciences and Natural Resources BGR, Stilleweg 2, 30655 Hannover, Germany

⁴ Nuclear Waste Management Organization NWMO, 22 St. Clair Ave. E., Toronto, ON, Canada

⁵ Federal Office of Topography swisstopo, 3084 Wabern, Switzerland

⁶ Solexperts AG, Mettlenbachstrasse 25, 8617 Mönchaltorf, Switzerland

⁷ Fracture Systems Ltd., Tregurrian, Ayr, St Ives, Cornwall, UK

⁸ Intera Incorporated, 1933 Jadwin Avenue, Suite 130, Richland, WA 99354, USA

⁹ Geomechanica Inc., 90 Adelaide St W, Toronto, ON M5H 4A6, Canada

¹⁰ TK Consult AG, Mainaustrasse 30, 8008 Zurich, Switzerland

Keywords Thermo-hydro-mechanical (THM) processes · Excavation damaged zone (EDZ) · EDZ self-sealing · Opalinus clay · THM modelling · Geological disposal of nuclear waste

Abbreviations

DECOVALEX	Development of coupled models and their validation against experiments
DFN	Discrete fracture network
EDZ	Excavation damaged zone
EPM	Equivalent porous medium
FDEM	Finite discrete element method
FORGE	Fate Of Repository Gases–EURATOM Collaborative Project/7th Framework Programme
GI1, 2 and 3	Long-term gas injection experiments in the HG-A experiment
NFPRO	Understanding and physical and numerical modeling of the key processes in the near field–EURATOM Integrated Project/6th Framework Programme
SA	Safety assessment
SF/HLW	Spent fuel/high level waste
SATP	Standard ambient temperature and pressure conditions (25 °C, 101 kPa)
TDR	Time domain reflectometer
THMC	Thermo-hydro-mechanical-chemical coupled processes
TIMODAZ	Thermal impact on the damaged zone around a radioactive waste disposal in clay host rocks EURATOM Collaborative Project/6th Framework Programme
NNW, SSE	Strike directions of the main tectonic fracture systems at Mont Terri CODE_BRIGHT, FLAC3D, TOUGH2, T2GGM are academic and commercial codes for THM modelling

1 Introduction

The construction of the underground facilities of a geological repository for radioactive waste, the emplacement of wastes during the operational phase, and the closure operations in different parts of the repository will induce perturbations of state variables (e.g. stress, water pressure, temperature, saturation, chemical composition of the pore-water) in the host rock around the underground structures. These perturbations are associated with several coupled thermo-hydro-mechanical-chemical phenomena (THMC). Within the zone where these perturbations occur there may

exist a zone of damaged rock. According to Tsang et al. (2005), the excavation damaged zone (EDZ) is a zone around the underground structures with significant irreversible processes and significant changes in flow and transport properties. These changes include, for example, one or more orders of magnitude increase in flow permeability.

In the framework of safety assessment (SA), a balanced evaluation of the impact of repository-induced effects on long-term safety is required. Such evaluation includes, but is not limited to, the role of the EDZ around the backfilled underground structures. The hydraulic significance of the EDZ as viable release path for radionuclides serves as a quantitative input for dose calculations. Furthermore, the EDZ may contribute in a beneficial way to repository performance as it represents an efficient pathway for the escape of repository gases associated with the corrosion and degradation of the wastes (see Nagra (2008) and Nagra (2016) for further details).

Dose calculations for SA require simplified abstractions of the EDZ. These abstractions represent the water/gas transport capacity of the EDZ after backfilling and sealing of the underground structures in terms of effective parameters for the thickness, hydraulic conductivity and porosity of the EDZ. It is common to describe the EDZ as a homogeneous circular shell around the backfilled tunnels (e.g. Lanyon and Senger 2011). Yet, robust assessments require a rigorous analysis of the associated conceptual and parametric uncertainties. Such analysis includes a detailed evaluation of the complete history of the EDZ, comprising its creation during repository construction, its evolution during the operational period and the post closure behaviour after backfilling of the underground structures. The shape and the extent of the EDZ are mainly controlled by the geological setting, initial state conditions (e.g. pore pressure, stress state), the excavation procedures and the design of the tunnel support system. The hydraulic significance of the excavation-induced release paths is affected by the action of the THMC phenomena and processes during the operational times and after repository closure.

Excavation damaged and disturbed zones have been studied in a range of rocks since the 1980s (Wilson et al. 1983). An early conceptualization of the EDZ in a low porosity marl formation (Helvetic Marls at the Wellenberg site in Central Switzerland) was presented in Nagra (1997). A comprehensive appraisal was dedicated to the creation and evolution of the EDZ in the Opalinus Clay formation at a repository depth of 650 m (Nagra 2002). In the EURATOM Integrated Project “NFPRO”, a state-of-the-art report on the creation and evolution of the EDZ was compiled, comprising a synopsis of experience from investigations in hard rocks, rock salt and clay formations (Alheid et al. 2007). The overall achievements of the

“NFPOR” research programme were summarized in the Final Synthesis Report (Aranyossy et al. 2008). More recently, a review of studies on the EDZ around excavations in sedimentary rocks was presented by Lanyon (2011). So far, full-scale investigations on EDZ development in indurated clays have been limited to the underground laboratories of Mont Terri (Lanyon et al. 2014), Tournemire (Rejeb et al. 2008) and the Meuse/Haute Marne site (Armand et al. 2013a, b).

Over the last two decades, the EDZ-related research programmes at the Mont Terri rock laboratory (Fig. 1) have gained recognition in the geoscientific community worldwide. As a result, new insights on the creation and evolution of the EDZ in indurated clays have seen light:

- Empirical evidence, contributing to the characterisation of the shape and extent of the EDZ for a variety of geological conditions, different excavation methods and tunnel support designs.
- Dedicated THMC experiments with emphasis on the phenomena and coupled processes governing flow and transport along the EDZ.
- Integrated experimental programmes providing qualitative and quantitative evidence of the gas and water transport capacity of the EDZ along seal sections of underground structures during all evolutionary stages.
- Complementary modelling programmes, aimed at the development and validation of traceable modelling workflows and simplified EDZ abstraction schemes.

The synopsis presented here refers to the key experiments at the Mont Terri rock laboratory in the fields of

EDZ related research and summarises distinguished achievements.

2 EDZ related phenomena and processes

2.1 Basic considerations

The nature and magnitude of excavation-induced damage around the underground structures of a geological repository evolve over time according to the life phase of the disposal system. Alheid et al. (2007) identified four major evolutionary phases, with corresponding phenomena and processes, in the context of the EC-funded project NFPOR: (i) the excavation phase, associated with coupled hydro-mechanical processes in the rock mass in response to mechanical unloading, (ii) the operational phase, affected by the ventilation of the underground structures, drainage of the rock mass and various perturbations due to operations in the repository, (iii) the backfilling and sealing of emplacement rooms, leading to resaturation of the unsaturated zone, heating effects around the high level waste (HLW) emplacement tunnels and coupled THM phenomena, and (iv) the repository closure phase, characterised by progressive resaturation of the host rock around the repository and saturation of the underground facilities, what induces chemical loadings able to amplify the interaction between chemical and mechanical processes.

Indurated clays such as the Opalinus Clay form a class of rock between soft rocks and hard clays. The strength of these rocks is relatively low, but tunneling is still feasible

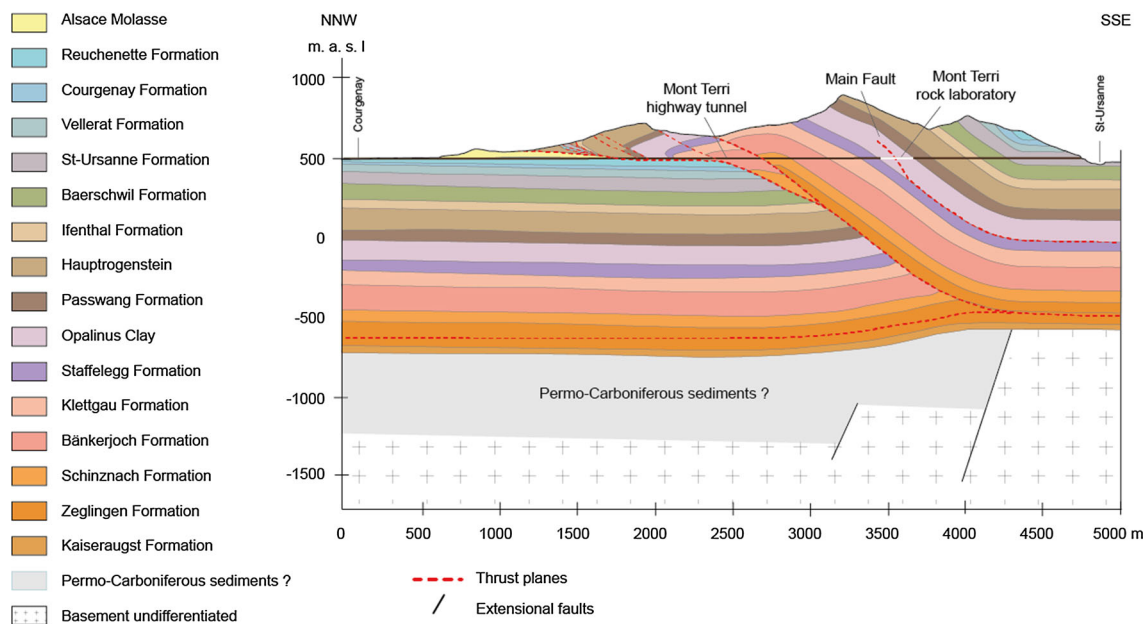


Fig. 1 Geological cross-section of the Mont Terri anticline and location of the Mont Terri rock laboratory (Nussbaum et al. 2017)

even with standard methods and low to medium support measures. The rock permeability is very low and even existing natural fractures do not show increased transmissivity as long as a significant normal stress is acting on the fracture surfaces. Similar to hard rocks (e.g. Martin et al. 2001) the stability of excavations can be considered under three classes:

- Structurally controlled failure (i.e. failure associated with reduced rock strength due to sedimentary and tectonic structures);
- Stress-controlled failure (i.e. failure associated with elevated deviator stress around the cavities);
- A combination of structure- and stress-controlled failure.

The application of such a failure classification scheme to clay-rich rocks is complicated by compaction processes, bedding-induced anisotropy and the influence of wetting. In this context, the following processes are of particular importance:

- Swelling, weakening and softening (see Steiner 1996 and Einstein 2002);
- Shrinkage during drying and loss of strength due to repeated wetting/drying cycles.

Structurally-controlled wedge-type failures can be managed by maintaining a compressive stress regime (Diederichs and Kaiser 1999) and identifying the relevant discontinuity sets. Yet, problems may occur at intersections

with other excavations or in regions with unexpected discontinuity orientations. Furthermore, within the repository, fault zones should be avoided in tunnel sections designated for seal emplacement. The focus for the EDZ-related studies is therefore on stress-controlled failure and combinations of stress/structure failure modes.

2.2 Phenomenology: empirical evidence

The creation and evolution of the EDZ around the openings is controlled by several factors, including the hydro-mechanical state conditions (e.g. stress, pore pressure, temperature), engineering design (e.g. configuration of the underground structures, size and shape of tunnel cross-sections, excavation technique, support system/lining) and the impacts on the system during the operational phase (e.g. ventilation, waste emplacement). The deformation behaviour is further complicated, amongst others, by (i) rock anisotropy (stiffness and strength), (ii) spatial variability of rock fabric (facies variability and tectonic features) and (iii) clay-specific hydro-mechanical couplings, giving rise to long-lasting time-dependent processes in the EDZ even after closure of the backfilled repository structures. Typical features of the rock mass fabric observed in the Opalinus Clay at Mont Terri are shown in Fig. 2. These include geostructural features observed at different scales, from the millimetre to the meter, and associated with both sedimentary and tectonic processes.

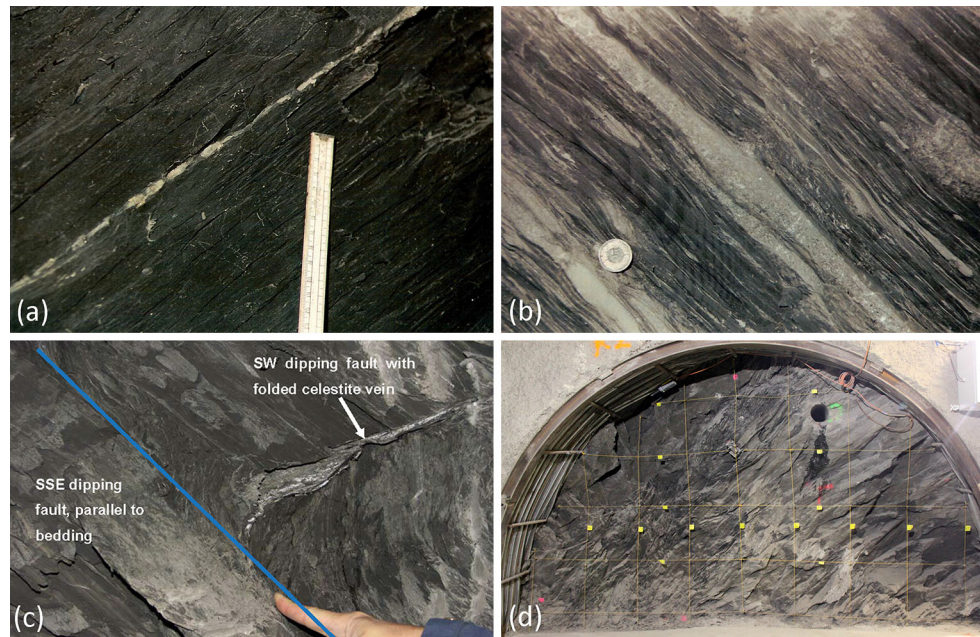


Fig. 2 Heterogeneity and anisotropy in the Opalinus Clay at Mont Terri (natural state): **a** dark grey silty, calcareous layers of the shaly facies with a vein of celestite; **b** silty to sandy marls of the sandy

facies with sandstone lenses cemented with carbonates; **c** SW dipping fault associated with a folded vein of celestite; **d** the Main Fault intersecting Gallery 98 in window through shotcrete

The inventory of brittle EDZ features (i.e., caused directly by the short-term excavation-induced unloading and loading) includes extensional fractures (Fig. 2a), spalling and buckling of the bedding planes (Fig. 2b, c), interactions with the existing tectonic features (Fig. 2b), bedding slip, single shear fractures and shear-bands (Fig. 3). Far reaching bounding shear bands delimit the EDZ and the intact rock zones (Blümling et al. 2007).

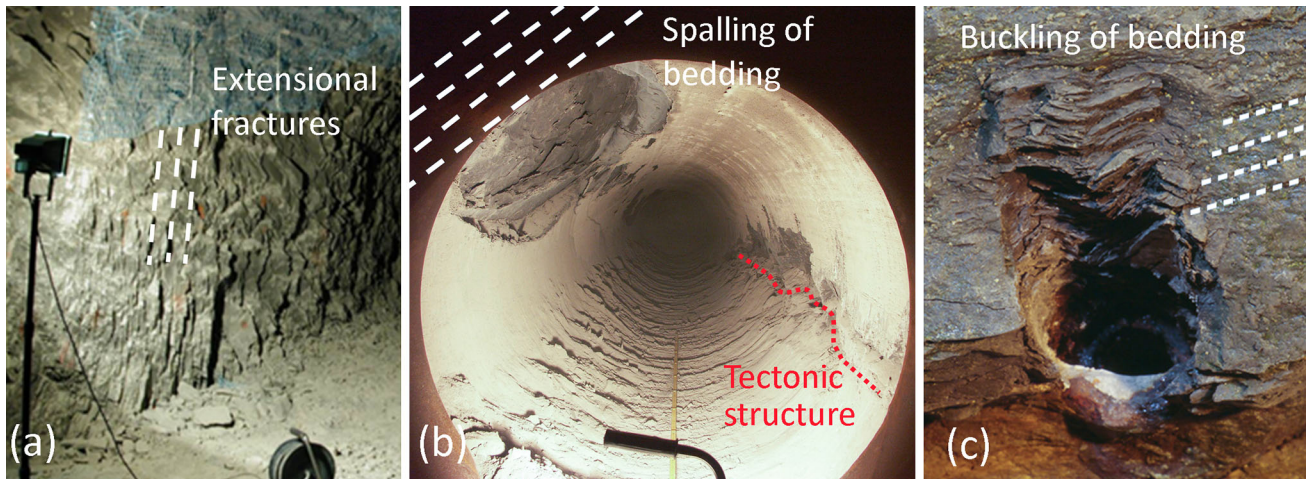


Fig. 3 Excavation-induced brittle features in Opalinus Clay (Mont Terri rock laboratory): **a** extensile fractures created during the excavation of Gallery 98 (Nagra 2002); **b** bedding related spalling processes in the crown of the HG-A microtunnel and interaction of

Further EDZ features can be attributed to the operational phase, such as desiccation cracks in response to tunnel ventilation and swelling-induced disaggregation of the rock matrix, when subjected to water-based fluids (e.g. cement water during the construction of the invert; water injections in boreholes, see Fig. 4a). In the Mont Terri rock laboratory, the prevailing ventilation conditions and the gravity driven pore-water drainage towards the tunnel system

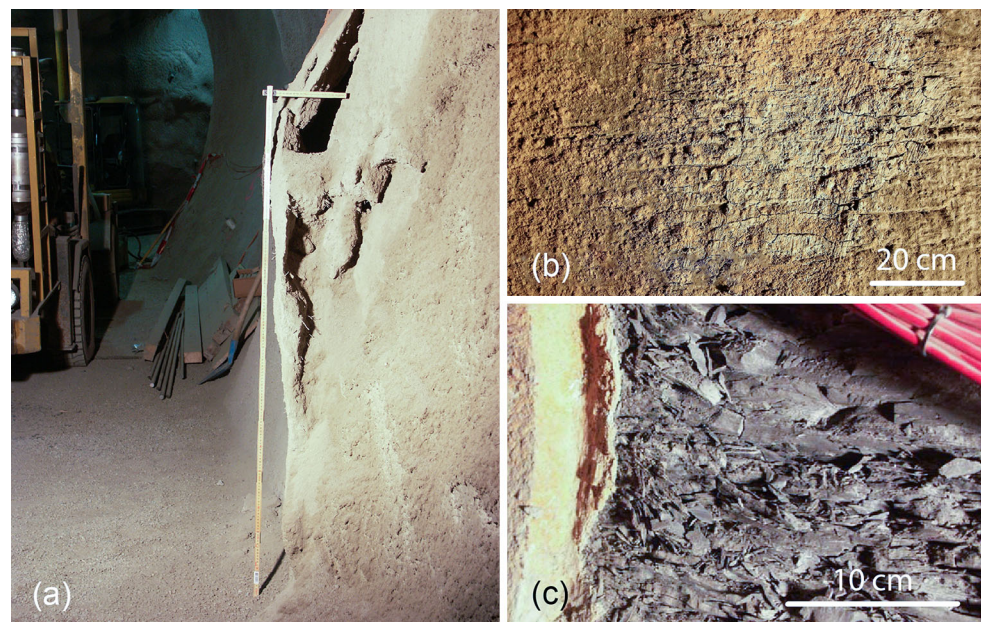


Fig. 4 EDZ-related phenomena in the Opalinus Clay during the operations phase of the Mont Terri rock laboratory: **a** damage of the shotcrete liner caused by swelling and creep processes; **b** dessication cracks at the tunnel wall of the HG-A microtunnel in response to

stress controlled failure at the lower right side wall with a tectonic structure (Marschall et al. 2006); **c** buckling of the bedding planes around a small borehole (Blümling et al. 2007)

tunnel ventilation; **c** degradation of the Opalinus Clay caused by water uptake at the contact zone between liner and rock (HG-A microtunnel)

cause a significant impact on the development of the EDZ. Cyclic deformation of the tunnel surface due to earth tides, as well as seasonal variations of barometric pressure, humidity and temperature lead to progressive degradation of the EDZ (Fig. 4b). Furthermore, monitoring and maintenance activities in support of the implementation of the in situ experiments may have increased the size of the EDZ in the long-term (e.g. water uptake during instrumentation of the HG-A tunnel; see Fig. 4c). In a real repository environment, there are further phenomena and processes, which may lead to a continuous weakening of the rock mass around the tunnel, such as ground motion associated with waste emplacement operations (successive excavation of emplacement tunnels, transportation of waste canisters, etc.). The weakening of the EDZ during the operational phase is associated predominantly with time-dependent ductile failure mechanisms (also termed “creep”), going along with a gradual loss of cohesion in the rock matrix and the development of fault gouges along fracture planes.

2.3 Extent of the EDZ and failure mechanisms

In the Mont Terri rock laboratory, the extent and shape of the EDZ have been characterized at various experimental sites using both geological and geophysical methods. Geological investigations include structural mapping of excavation surfaces (tunnel walls, niches and wallrock “windows”) and core mapping of boreholes drilled from the excavation (most commonly radial boreholes). Classification schemes were established to discriminate between natural (tectonic) fractures and faults, EDZ-related features and artificially induced fractures caused by drilling and core handling.

Structural mapping of the tunnel walls of the newly excavated cavities has been a routine procedure associated with all previous extensions of the Mont Terri rock laboratory. In addition, dedicated experimental programmes were initiated to characterise in a systematic way the shape and extent of the EDZ and to establish inventories of EDZ features for tunnel sections parallel and normal to bedding. A comprehensive compilation of the corresponding structural data bases is given in Lanyon et al. (2014), comprising structural maps and structural analyses of core samples from the EZ-A niche, Gallery 04, EZ-B niche, HG-A microtunnel, Gallery 08, Mine-By Experiment and the FE-Experiment. The compilation refers—amongst other aspects—to the detailed evaluation of EDZ fracture statistics by Yong (2007), which draws on elaborate analysis of fracture density from over 100 boreholes (see Fig. 5). Yong’s evaluations reveal that fracture count in the first 0.5 m can be as high as 10 (mean spacing of 5 cm between fractures) around some excavations but typically reduces to less than 2 between 2.5 and 3 m from the tunnel

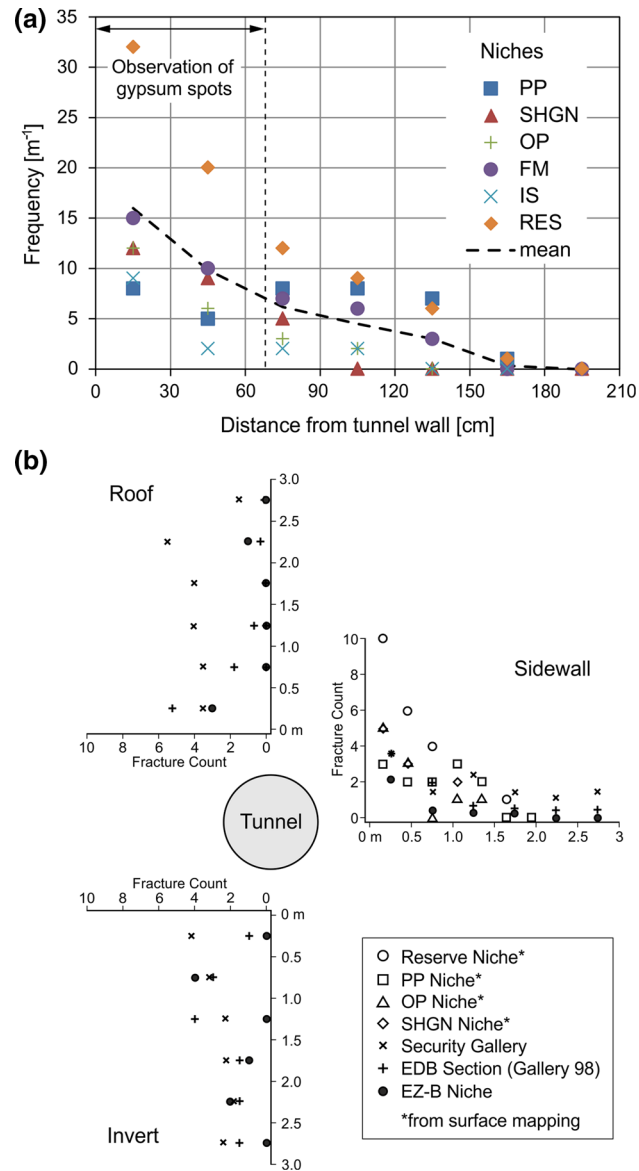


Fig. 5 Fracture statistics derived from tunnel mapping and borehole logging: **a** line-counted frequencies from the side walls of the niches in the security gallery (after Bossart et al. 2002) and **b** fracture counts in 0.5 m borehole intervals from the EZ-B Niche and previous sub-parallel excavations (from Yong 2007)

wall. Detailed investigation of macro-fracturing around the EZ-B niche suggested a much narrower zone of macro-fracturing with a thickness of ~20 cm and an outer zone extending to 70 cm characterised by a reduced seismic velocity. Almost all excavations show the highest fracture density close to the tunnel wall and significant drop in fracture frequency beyond 2 m from it.

Another method for core mapping developed at Mont Terri involves resin injection into a pilot hole followed by subsequent overcoring (Bossart et al. 2002, 2004). The resin injection method allows one to identify open (resin-impregnated) fractures within the EDZ and can give

information on the prevailing fracture mechanisms, reactivation of pre-existing features, connectivity and structural relationships. Labrouse and Vietor (2014) used this method in the context of the EC-funded TIMODAZ project (SE-H experiment) for analysing an overcore from a sub-horizontal 101 mm borehole, which had been used for a 3 year-long dilatometer test. Resin-impregnated core samples (Fig. 6a) corresponding to the test and packer sections show similar fracture patterns, indicating that the mechanisms leading to borehole collapse were similar and independent of the testing history. The sub-vertical buckling failure zones extend beyond the overcore (in excess of a borehole diameter).

The fracture mechanisms postulated by Labrouse and Vietor (2014) on the borehole scale exhibit distinct similarities with the conceptual model developed by Martin and Lanyon (2003) for the EDZ around the EDB section of Gallery 98. Extensional fractures formed in the excavation side-walls while the EDZ in the roof and floor was related to a region of potential bedding-slip and subsequent kink/buckling failures (see Fig. 6b). Blümeling et al. (2007) further developed the model of Martin and Lanyon (2003), incorporating the observed buckling failure and through-going shears associated with bedding slip.

The aforementioned characterisation methods are complementary in the sense that different emphasis is placed on

various aspects of the EDZ and excavation orientation. In the past, numerous conceptual EDZ models have been developed for the Mont Terri rock laboratory, capable to explain the prevailing structural features and failure mechanisms for particular geological settings and a given excavation method. Thus, for excavations normal to bedding strike (i.e., sub-parallel to σ_{hmax}), Bossart et al. (2002) present a concept of “onion-like” extensile fractures forming an interconnected network within 1 m from the tunnel wall but tending to be isolated structures beyond this distance (Fig. 7a). For the same orientation of the excavation, Blümeling et al. (2007) complement the concept of extensile fracturing by adding buckling and kink failures, commonly associated with zones of bedding slip and multiple through-going shears (Fig. 7b). Complex combinations of structural and stress induced failure (Fig. 7c) have been conceptualised by Marschall et al. (2006) for excavations along bedding strike (i.e., sub-parallel to σ_{hmin}).

The complexity of the geological setting (stress state, lithological variability, tectonic overprint) and the differences in the adopted excavation approaches makes it challenging to develop a generalised conceptual model of the EDZ at Mont Terri. Nevertheless, important conclusions can be drawn with respect to the inventory of characteristic EDZ features and the EDZ related phenomena and processes:

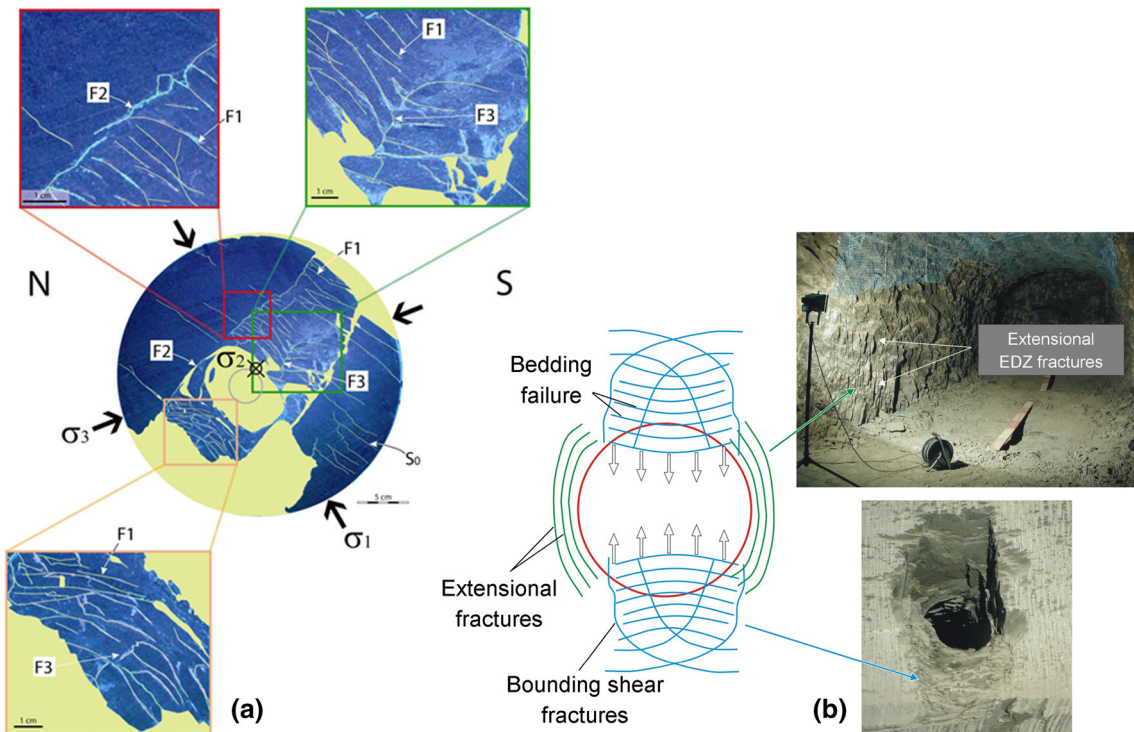


Fig. 6 Fracture mechanisms postulated by Labrouse and Vietor (2014): **a** analysis of resin impregnated core samples (SE-H project), **b** conceptual model of fracture mechanisms at the tunnel scale,

developed by Martin and Lanyon (2003) for the EDZ around the EDB section of Gallery 98

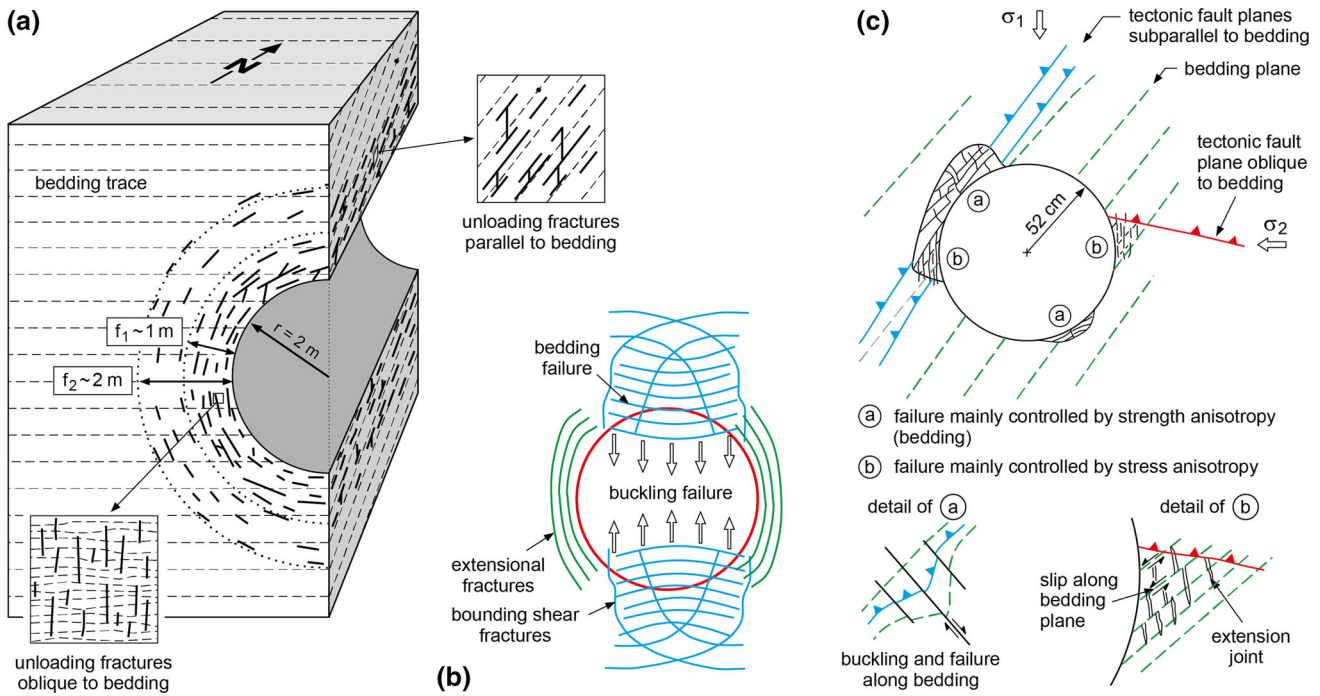


Fig. 7 Conceptual models of EDZ, derived in the framework of Mont Terri Project: **a** radial distribution of extensile fracturing (tunnel axis normal to bedding strike, sub-parallel to σ_{hmax} ; see also Bossart et al. 2002); **b** combined buckling failure and extensile fracturing (tunnel axis normal to bedding strike, sub-parallel to σ_{hmax} ; see also Blümling

et al. 2007); **c** schematic representation of the damage zone around the HG-A microtunnel, showing the key processes and features that affect borehole stability: slablike breakouts on the *upper left side* are caused by extensile failure along tectonic fractures and wedge-like breakouts on the *right side*

- Clear evidence was found, that the immediate (short-term) failure of the Opalinus Clay in response to the excavation process is brittle. The inventory of EDZ-related features can be classified as extensional fracturing, bedding parallel slip, buckling and kink failures, single shear fractures and shear bands and, eventually, reactivated tectonic features.
- The short-term response can be stress controlled, structurally controlled or a combination of both regimes.
- Governing parameters for stress controlled failure are the in situ stress tensor and the stress state ahead of the tunnel face. Thus, stress controlled failure is strongly related to the adopted excavation techniques and the progress of excavation.
- Structurally controlled failure is caused by sedimentary and tectonic structures. Variabilities in microstructure such as bedding or intercalations of sandy and clay-rich layers tend to create self-similar failure patterns (e.g. buckling), which are observed at scales ranging from small boreholes to the tunnel scale (see Fig. 3). In addition, reactivations of tectonic structures are highly irregular and, consequently, difficult to predict without detailed knowledge of the pre-existing fracture patterns.

- The long-term response of the rock during the operational phase in terms of tunnel convergence is largely associated with ductile failure mechanisms and can be conceptualised as a viscous component (termed “creep”) in the deformation behaviour of the rock.

2.4 Hydraulic characterisation of the EDZ

Representative transmissivity estimates of the EDZ fractures immediately after excavation are of high importance for the calibration of discrete fracture network models (DFN models; see Alcolea et al. 2016). To that end, small-scale in situ transmissivity measurements were carried out in radially oriented boreholes as part of the early EDZ related research programme (Bossart et al. 2002). The boreholes were equipped with multi-packer systems, isolating measurement intervals of 10–50 cm at various distances from the tunnel wall. Hydraulic pulse and constant head tests were conducted in the saturated part of the EDZ, whereas simple pneumatic tests were undertaken in the unsaturated rock in the immediate vicinity of the tunnel surface to investigate the local effective permeability. Figure 8 shows that permeability increases several orders of magnitude (up to 6–7) within 20–40 cm from the tunnel.

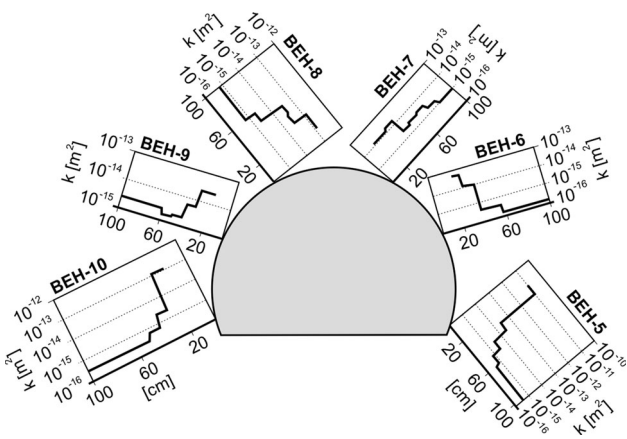


Fig. 8 Hydraulic characterisation of the EDZ features around excavations in the Mont Terri rock laboratory: in-situ permeability measurements conducted in Mont Terri experimental drift (from Bossart et al. 2002)

This zone coincides with that exhibiting high fracture density.

Several experiments were conducted to demonstrate the evolution of transmissivity of the excavation-induced fractures in the ventilated tunnel and after re-compaction of the EDZ in order to capture the time dependence of the self-sealing process. A long-term in situ experiment, conducted in the EDZ of an open tunnel section, indicated a significant reduction of the EDZ transmissivity over a period of 800 days from 5×10^{-7} to $2 \times 10^{-9} \text{ m}^2/\text{s}$ (blue dots in Fig. 9). During the subsequent test phase, a load plate was installed and the EDZ was subjected to radial stresses between 1 and 5 MPa to simulate bentonite swelling pressures in a backfilled emplacement tunnel. A further drop in transmissivity of two orders of magnitude to $2 \times 10^{-11} \text{ m}^2/\text{s}$ was observed (red dots in Fig. 9).

2.5 Investigation of fracture closure mechanisms

The dependence of fracture transmissivity on effective normal stress has been the issue of laboratory studies and in situ tests (Blümling et al. 2007). As part of the GS experiment (Gasfrac Self-sealing) at Mont Terri, hydraulic tests were performed in a borehole before and after a combined hydro- and gas-fracture experiment (Marschall et al. 2005). The experiment was carried out in a test interval containing a hydrofrac with a well-defined fracture geometry. Interval transmissivity increased by 5–6 orders of magnitude when the injection pressure exceeded the effective normal stress on the fracture plane (Fig. 10). For low injection pressures, however, the interval transmissivity was close to that of the intact rock ($T \leq 10^{-12} \text{ m}^2/\text{s}$). These findings can be explained by the dependence of fracture transmissivity (or hydraulic conductivity) on effective normal stress, which follows a hyperbolic fracture

closure law (see Nagra 2002). An effective mechanical self-sealing of the artificial fracture is observed already at moderate effective normal stresses in the order of 1–2 MPa (Fig. 10).

3 Modelling of water/gas flow along the EDZ

3.1 Background and rationale

The complexity of the hydro-mechanical phenomena associated with the creation and temporal evolution of the EDZ precludes a detailed representation of the EDZ with conventional modelling tools for safety assessment (SA). Therefore, quantitative analyses in support of the assessment of long-term radiological safety of geological repositories are often based upon simplified representations of the EDZ, assuming a configuration of concentric shells (single or double shell) with enhanced hydraulic conductivity (Fig. 11).

In recent years, several numerical EDZ abstraction approaches have been proposed for SA applications, referring to data bases from the Mont Terri rock laboratory. Lanyon and Senger (2011) developed a sequential modelling approach for indurated clay formations, based on a stochastic representation of the EDZ in terms of discrete fracture network (DFN) models. The underlying hydraulic DFN models, derived from structural mapping of tunnel walls and drillcores, were converted into equivalent porous medium (EPM) models with stochastic permeability distributions. Combined water and gas flow along stochastic realizations of the EDZ was simulated with the EPM models. Eventually, effective properties suitable for performance assessment were derived by inverse modelling of the results of stochastic modelling with a simple single shell representation of the EDZ. Senger et al. (2013) validated the aforementioned modelling approach with long-term monitoring data from the HG-A experiment (gas path through host rock and along seals) at Mont Terri.

Walsh et al. (2015) developed an EPM-based modelling framework which simulates two-phase flow with the T2GGM code (Suckling et al. 2012) and mechanical processes with FLAC3D (Itasca 2012). This coupled model predicted the evolution of the EDZ around the HG-A tunnel, and then modelled the EDZ permeability as a function of time (self-sealing) and packer pressure (hydro-mechanical coupling).

Alcoverro et al. (2014) developed a simplified hydro-mechanical modelling approach for SA applications using the THM-simulator CODE_BRIGHT (DIT-UPC 2000). The permeability of the EDZ was assumed to depend on deformation, allowing the simulation of self-sealing processes in the EDZ in response to re-saturation and stress

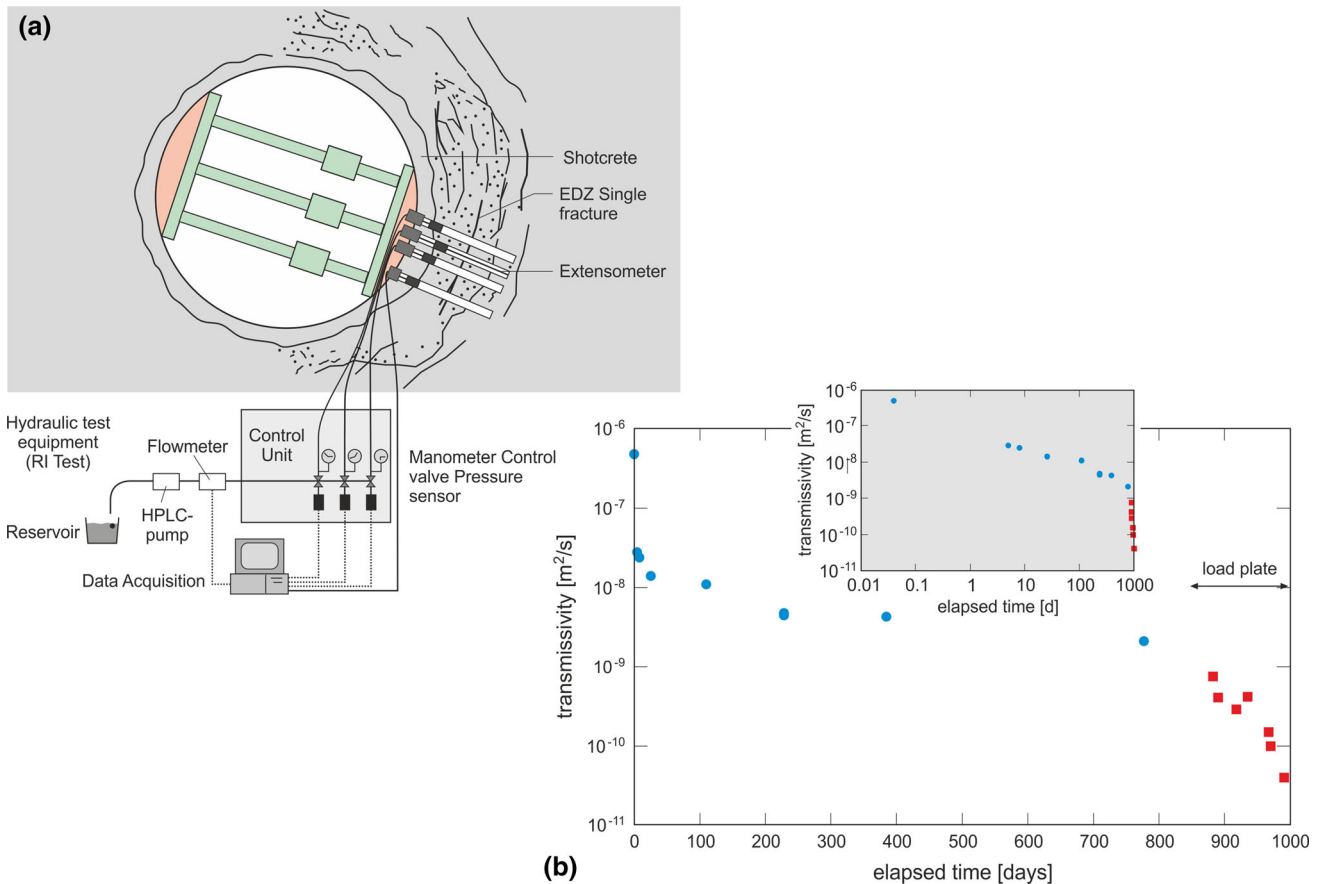
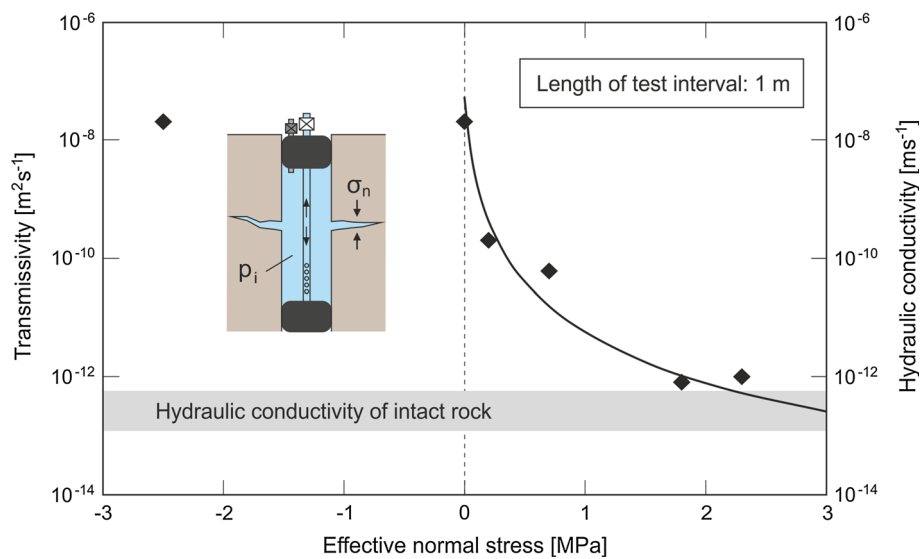


Fig. 9 Long-term changes in EDZ transmissivity in an open tunnel section at the Mont Terri rock laboratory: **a** sketch of the experimental set-up and **b** long-term monitoring of EDZ transmissivity. Initially, the EDZ was saturated for a period of 800 days (blue dots) and EDZ

transmissivity was monitored periodically. Afterwards, a load plate inducing a radial stress between 1 and 5 MPa was installed and the transmissivity measurements were repeated (EU Selfrac Project; Nagra 2002)

Fig. 10 Experimental evidence of sealing effects in Opalinus Clay at Mont Terri. Suggested hyperbolic relationship between interval transmissivity and effective normal stress, $(\sigma_n - p_i)$, based on the investigation of fracture closure mechanisms in the so-called Gasfrac self-sealing (GS) experiment (after Nagra 2002). Hydraulic tests were conducted for different interval pressure values, p_i . The normal stress, σ_n (ca. 4.3 MPa), was derived from the shut-in pressure recorded during hydraulic fracturing



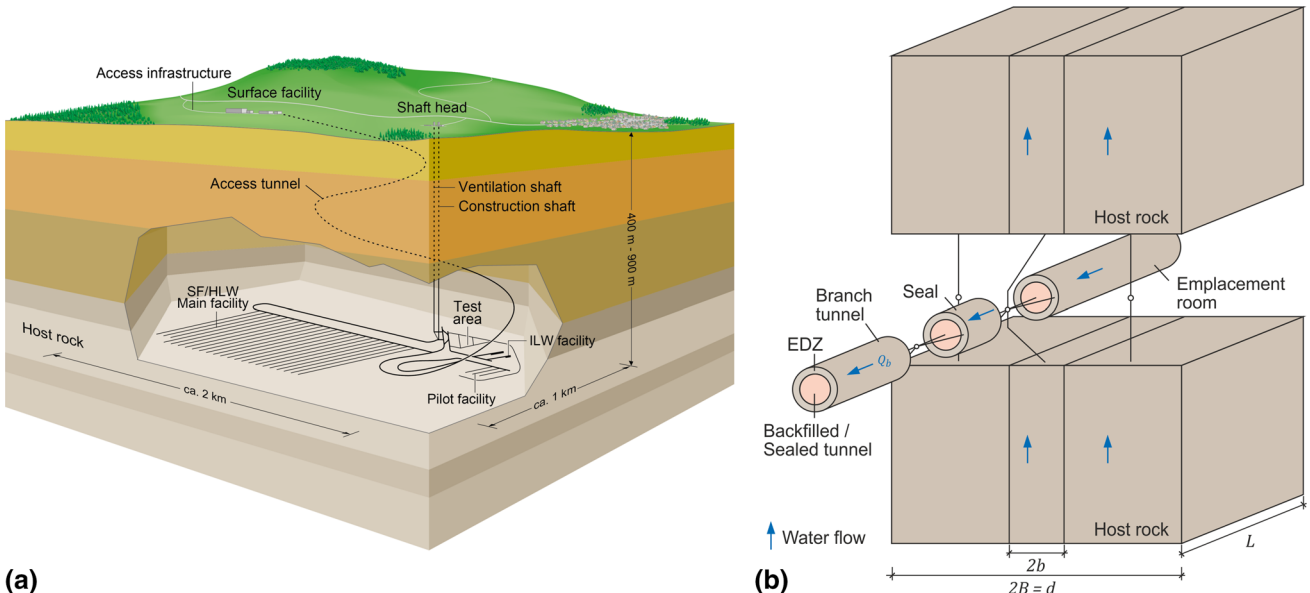


Fig. 11 Simulation of radionuclide release in safety assessment (SA): abstraction of the radionuclide release paths from the site descriptive model (*left*) towards a simplified representation in a numerical

recovery. The modelling approach was benchmarked extensively with long-term monitoring data from the HG-A experiment.

3.2 A novel EDZ abstraction approach

The aforementioned EDZ modelling approaches have successfully demonstrated their suitability for simulating the hydraulic behavior of the EDZ around backfilled tunnel sections and for the back-analysis of the self-sealing processes associated with the re-saturation and pressure recovery along the seal section of the HG-A experiment. A shortfall of these approaches is their limited ability to represent the mechanisms of fracture closure in response to pressure recovery in the EDZ, thus restricting the predictive capability of the models.

A novel numerical approach has been developed by Alcolea et al. (2016) with special emphasis on an adequate representation of the hydro-mechanical conditions in the EDZ, covering the full range of hydraulic regimes, from the fracture dominated, with localised pore-water flow during early times, to the matrix-dominated distributed flow in the late times. The workflow consists of three main steps carried out sequentially (Fig. 12). First, a hybrid finite-discrete element method (FDEM; Lisjak et al. 2016) is used to simulate the geometry and geomechanical conditions of the discrete fracture networks forming the EDZ (Fig. 12a). The FDEM simulations are purely mechanical and mimic the excavation and emplacement processes only. Second, the geometric properties simulated by the

transport code (*right*). The EDZ is implemented as a single shell model with effective properties in terms of cross-sectional area, porosity and hydraulic conductivity (modified after Poller et al. 2014)

FDEM are mapped onto a finite element mesh (Fig. 12b), which allows to solve the fluid motion equations in the excavation near-field. A salient feature of the suggested approach is that hydraulic parameters of both fracture and matrix evolve over time as a response to re-saturation of the tunnel surroundings. Finally, an abstraction of the complex model is made based on the late time behaviour (after full re-saturation) of the system (Fig. 12c). The main outputs of the model are the spatio-temporal distributions of hydraulic parameters and the corresponding specific fluxes towards the tunnel, with special emphasis on the late time behaviour. Finally, the abstraction of the EDZ is implemented by defining a piece-wise homogeneous “shell-like” model with hydraulic behaviour identical to that of the complex model.

3.3 Heuristic modelling concept of fracture self-sealing

Based on the presented empirical and experimental evidence (Sect. 2), the hydraulic significance of the EDZ during tunnel construction and its evolution during the operational phase and after backfilling of the underground structures can be formulated in terms of a heuristic EDZ closure model (Fig. 13). The creation of the EDZ is a brittle process, i.e., the increase of the void volume in the damaged rock zone around the excavation is solely attributed to fracture opening, whereas the porosity of non-fractured rock remains essentially unchanged during the early times after excavation. Initially, the newly created

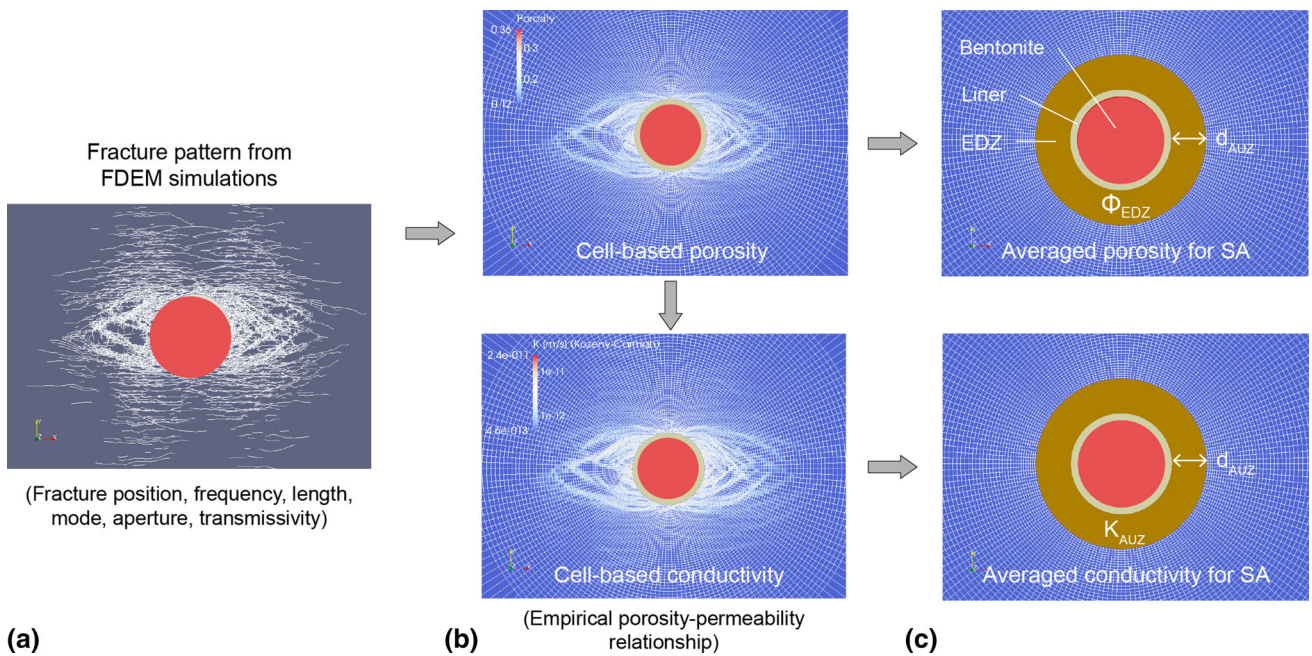


Fig. 12 Concept of the EDZ abstraction procedure for safety assessment (SA) applicable for a circular tunnel (after Alcolea et al. 2016): **a** representative fracture patterns are simulated for relevant repository configurations with a discrete element model (FDEM); **b** the discrete fracture patterns are converted in heterogeneous

porosity and hydraulic conductivity distributions; **c** in a final abstraction process, the heterogeneous porosity and conductivity distributions are converted into a shell defined by a radius and homogeneous porosity and conductivity

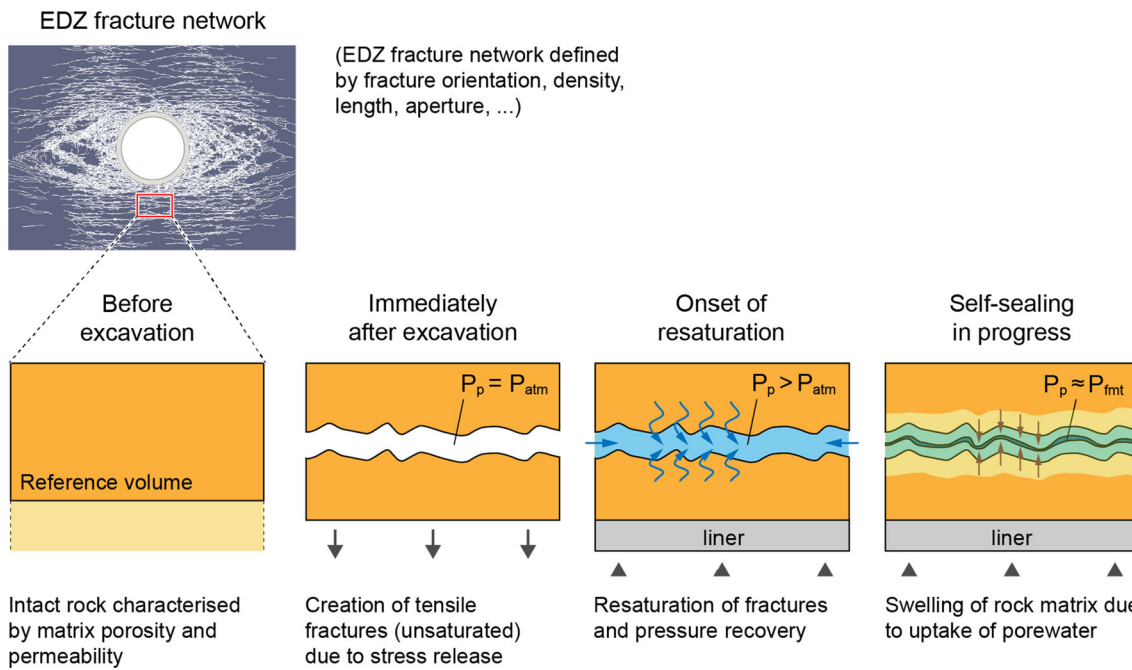


Fig. 13 Schematic sketch of the conceptual framework for EDZ fracture closure in Opalinus Clay, covering the key phenomena and features from the early post excavation phase until static formation pressure recovery

EDZ fractures are unsaturated and exposed to atmospheric pressure, whereas the non-fractured rock remains saturated and exhibits high matrix suction as a consequence of the high gas entry pressure of the Opalinus Clay (Ferrari et al.

2014). The initial transmissivity of the unsaturated EDZ fractures is controlled by the fracture aperture and can be very high. The matrix conductivity remains essentially unchanged, i.e., it is the same as the conductivity of the

intact rock. With time, the matric suction in the rock matrix decreases due to the uptake of pore-water from outer rock zones and the fractures start to resaturate. Pore-water uptake from the non-fractured rock zones is associated with swelling and consequently with an increase of matrix porosity. This porosity increase occurs at the expense of a decrease of fracture aperture (and correspondingly, of fracture transmissivity), i.e., fractures start to close and fracture transmissivity reduces drastically, whereas the hydraulic conductivity of the non-fractured matrix zones increases slightly as a consequence of the porosity increase. This process continues until the equilibrium of effective stresses is reached. This is essentially the case, when pore pressure reaches the static formation pressure.

Alcolea et al. (2016) implemented the heuristic EDZ closure model in a numerical workflow and subjected long-term monitoring data from the HG-A experiment at Mont Terri to a detailed back analysis. The results of this analysis are presented in the subsequent paragraphs.

4 Assessment of model performance

4.1 The role of the Mont Terri rock laboratory

The performance of a modelling approach is commonly evaluated by comparing model predictions with experimental evidence. Rigorous model validations require comprehensive benchmark exercises for the full range of intended model applications as part of a systematic prediction-evaluation process. In geoscientific modelling workflows rigorous validations are rarely achieved due to the lack of detailed knowledge concerning the actual state of the modelled geo-system and the limited amount of measurements of its temporal evolution. In this sense, the Mont Terri rock laboratory offers a unique opportunity to collect comprehensive geoscientific data bases for model validation not only from well-instrumented long-term in situ experiments, but also from general site characterisation activities such as structural mapping and borehole logging.

Modelling benchmarks for the simulation of the hydro-mechanical evolution of the EDZ have been carried out as part of the EC-funded FORGE project (Harrington et al. 2013; Shao et al. 2015) and in the framework of the DECOVALEX project (Xu et al. 2013; Nguyen and Le 2015). In both benchmark exercises, the HG-A in situ experiment at Mont Terri served as a key experiment for model calibration and validation.

4.2 The HG-A experiment

The HG-A experiment (gas path through host rock and along seal sections) was designed as an integrated

experimental programme to provide qualitative and quantitative evidence of the gas and water transport capacity of the EDZ along the sealed section of the HG-A microtunnel during all relevant evolutionary stages, comprising the excavation phase, a short ventilation period and the backfilling and sealing stages (Marschall et al. 2006, 2008; Lanyon et al. 2009, 2014). The test site is located in the southern part of the Mont Terri rock laboratory off Gallery 04 (Fig. 14). A 1 m diameter, 13 m long microtunnel was excavated during February 2005 from a niche in Gallery 04. The microtunnel was directed parallel to bedding strike and bedding parallel features run along the tunnel. Excavation was monitored by a borehole array containing piezometers and deformation gauges (clino-chain and chain deflectometers). The borehole array was subsequently augmented with additional piezometer boreholes and borehole stressmeters.

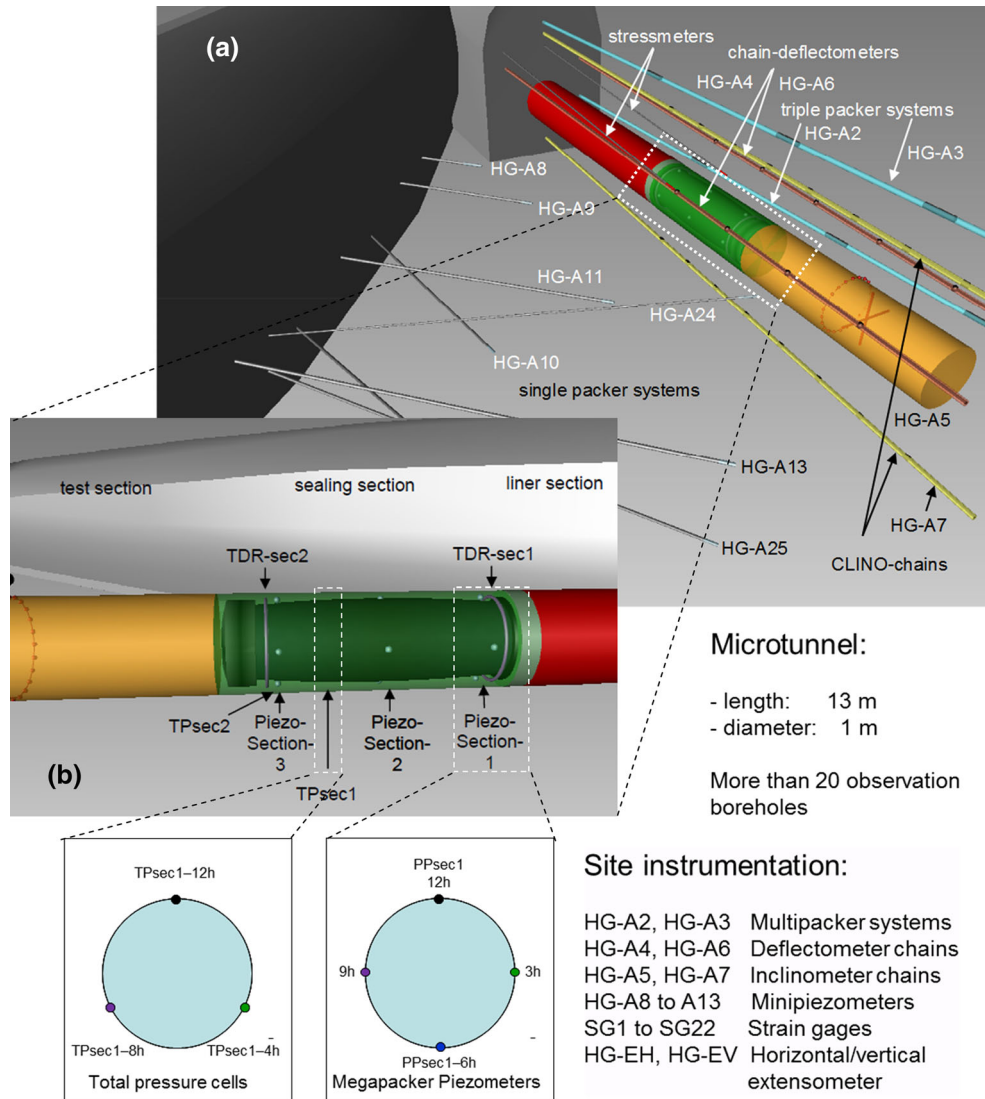
4.3 Creation of the EDZ

The excavation of the HG-A microtunnel was carried out using a steel auger (Marschall et al. 2006). No drilling fluid was used in order to avoid swelling and disaggregation of the clay during drilling. Immediately after termination of the drilling process, a steel liner was installed along the first 6 m of the microtunnel to stabilise the damage zone around the tunnel entrance. Detailed small scale geological mapping of the tunnel section between 6 and 13 m was carried out after emplacement of the liner. The facies in the microtunnel is composed of marly shales, which are locally intercalated with grey-white silty limestones and weakly cemented fine-grained brownish siderite layers. On the metre scale, the lithologies are quite homogeneous. However, a quite pronounced bedding anisotropy could be mapped (bedding traces in the microtunnel are almost horizontal, true bedding dip is 51°).

After completion of construction, the surface of the microtunnel was scanned with a tachymeter from 6 to 13 m along the tunnel axis (Fig. 15), which confirmed the results of structural mapping, indicating that breakouts occur mainly at locations where bedding is oriented tangential to the tunnel circumference.

The instantaneous brittle failure process during and immediately after excavation of the HG-A microtunnel exhibits the characteristic EDZ features around cylindrical cavities in claystone formations, such as massive breakouts, spalling and buckling phenomena. Instantaneous failure was caused by the combined effect of (i) the anisotropy in far-field stress, (ii) the anisotropy of geomechanical rock properties (stiffness and strength) and (iii) the heterogeneity of the rock mass (tectonic fracture systems and flaws in the rock fabric). The conceptualisation of the damage zone around the HG-A microtunnel (Marschall

Fig. 14 Schematic drawing of the HG-A microtunnel and the site instrumentation. Colour coding refers to the steel liner (red), the seal section (green) and the backfilled test section (orange)



et al. 2006) is given in Fig. 7c. The damage zones on the upper left side (9:00–11:00 o'clock) exhibit clear signatures of extensile fracturing such as plumose structures and disjoining of bedding planes. The breakouts are largely linked to the SSE dipping thrust system, which is oriented subparallel to the bedding planes and intersects the tunnel at a low angle. These fractures represent planes of weakness with reduced uniaxial compressive strength and are therefore preferential loci for failure initiation during the excavation process. In the upper zone between 10:00 and 11:00 o'clock, spalling and buckling phenomena create slab-like breakouts. Spalling occurs preferentially in the rear end of the tunnel at areas where SSW dipping fault planes phase out, whereas buckling dominates in the section with the most prominent breakouts between 6 and 9 m. In the lower zone between 9:00 and 10:00 o'clock, damage seems more and more stress controlled, i.e., onion-like extension joints associated with the minor in-plane

principal stress component tend to delimit the damage zones on the left side of the tunnel. Less distinct are the buckling phenomena along the tunnel floor (about 5:00 o'clock). No significant breakouts are formed in this zone, because the debris is kept in place due to gravity. Complementary extensometer records give clear indication for on-going tunnel convergence in the lower sidewall to the NNW.

4.4 Hydraulic and gas testing

Following a short ventilation phase of several months, the test section (9–13 m) and the seal section (6–9 m) of the microtunnel were instrumented with piezometers, extensometers, strain-gauges, total pressure cells and time domain reflectometers (TDRs) to measure pressure, deformation, total stress and water content. Finally, the megapacker was installed in June 2006. Saturation of the

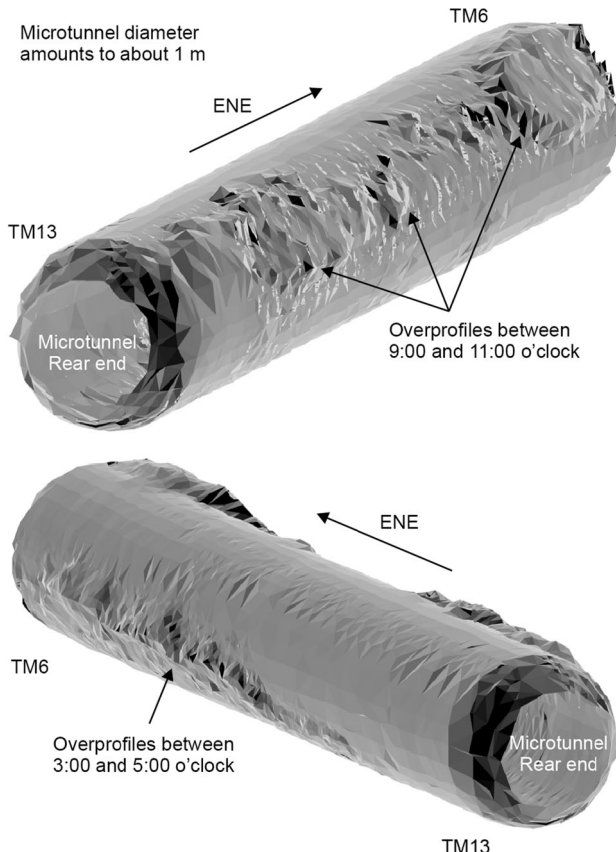


Fig. 15 Characterisation of the EDZ in the HG-A microtunnel: 3-D laser scan with a tachymeter. Views are from the rear end of the tunnel towards the SSE side wall (*top*) and the NNW side wall (*bottom*), respectively. The radial accuracy of the scans is ± 3 mm and the axial resolution varies between 5 and 10 cm

test section and surrounding rock started in November 2006 and comprised several saturation tests and a long-term multirate hydraulic test, starting in January 2008 (Fig. 16). This test continued until February 2010 and involved a series of constant rate injection steps, with stepwise reduced rates in the range between ca. 10 and 0.1 ml/min. The results from the hydraulic testing indicated progressive self-sealing (Lanyon et al. 2014). During hydraulic testing the effective stress conditions in the seal zone were altered by varying the megapacker pressure in the range between 2000 and 2600 kPa.

The gas injection phase included three separate nitrogen gas injections termed GI1, GI2 and GI3. Figure 16 displays the corresponding microtunnel sensor responses. After each gas injection, following a shut-in period, water was extracted from the test section and depressurized to remove trapped gas (gas–water exchange). The degassed water was then re-injected into the test section. This procedure provided a well-defined initial gas saturation in the test section pore-water for the subsequent gas injection. During gas injection a low constant rate (c. 0.02 ml/min) water

injection was maintained in the test section. Gas pressure during GI1 was limited to 1200 kPa, significantly below the minimum stress, to avoid coupled mechanical effects. After an initial 20 ml/min (SATP) injection, when pressure rose quickly, the injection rate was reduced to about 10 ml/min (SATP) to maintain an approximately constant pressure in the test section. During GI2 test section pressure rose more slowly than in GI1 and then peaked at around 1350 kPa. After the pressure breakdown, the test section pressure dropped over about a month by ca. 350–1000 kPa and then stabilized at about 1040 kPa. During GI3, test section pressure again peaked at 1350 kPa but with a broader peak than in GI2 and then dropped to about 850 kPa owing to an interruption in injection before recovering (after resumption of gas injection) and stabilised at about 1000 kPa.

4.5 Modelling of EDZ formation

Lisjak et al. (2016) carried out numerical simulations of the EDZ formation and compressive stress controlled sealing process around the HG-A microtunnel using a hybrid finite-discrete element method (FDEM). The model geometry consisted of a circular opening representing a 2D cross section of the HG-A microtunnel located along the seal section (Fig. 17). The influence of model boundaries on the excavation near-field was minimized by placing them at a distance of 10 m from the centre of the microtunnel. To maximize the model resolution in the EDZ while keeping the computation times within practical limits, a $4\text{ m} \times 4\text{ m}$ mesh refinement zone, with a nominal element size of 0.015 m, was adopted around the excavation boundary. In this zone, the mesh was pre-conditioned along the bedding direction by introducing a layering thickness of 0.05 m, as required to adopt the anisotropic fracture model. A transversely isotropic stiffness model coupled with a direction-dependent fracture criterion was adopted for the Opalinus Clay. The input values for the fracture model were derived from the FDEM back-analysis of the full-scale emplacement (FE) tunnel at the Mont Terri rock laboratory (Lisjak et al. 2015). The reference values of the principal stress components at Mont Terri ($\sigma_1 = 6.5$ MPa, $\sigma_2 = 4.5$ MPa, $\sigma_3 = 2.5$ MPa) were used to specify the in situ stress field in the HG-A model.

The simulation of the EDZ formation and recompaction process was accomplished with two separate model runs. The first run was intended to analyse the failure mechanisms and damage propagation associated with the EDZ formation process. The second run was dedicated to the recompaction of the EDZ in response to packer inflation, acting as a radial stress on the inner model boundary.

A total of 5 model variants were specified as part of a sensitivity analysis, aimed at assessing the impact of

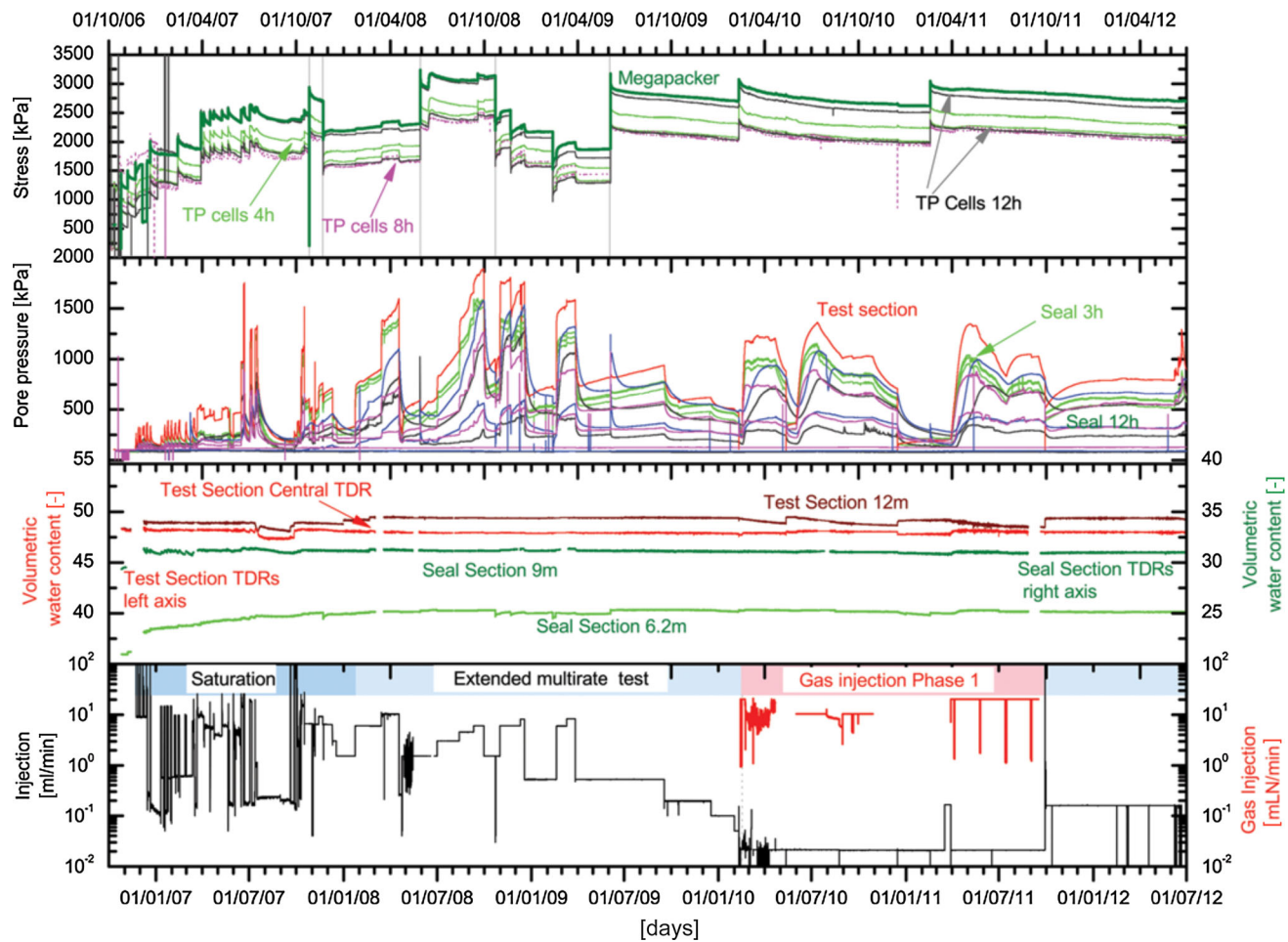


Fig. 16 Microtunnel stress, pore pressure, water content and flow rate measurements from start of saturation (from Lanyon et al. 2014)

parametric and conceptual uncertainties on the EDZ formation. Of particular interest was the effect of the tectonic fault (see Fig. 7c) on the development of the EDZ fracture pattern. The numerical results of the model variant with tectonic fault (model “HG-A-F”) indicate that damage starts to develop around the excavation boundary in response to the gradual softening of the excavation core (Fig. 17). Failure initiates in the form of shear (i.e., Mode II) fractures nucleating and growing along bedding planes approximately tangential to the tunnel walls (Fig. 17a,b). The distinctive location of these failure zones is caused by a combination of compressive stress concentration arising in the sidewalls and the low shear strength of the bedding planes. The impact of the tectonic discontinuity with fault plane oriented oblique to bedding affects the rock mass strength, fracturing behaviour, as well as the induced failure kinematics in the subsequent phases of damage propagation (Fig. 17c, d). A distinctive interaction can be observed between the pre-existing discontinuity in the right sidewall and the growing EDZ fractures. Particularly, the propagation of shear fractures nucleating at 270°–360°,

tends to be arrested at the intersection with the fault plane (Fig. 17c). As a result, the growth of shear fractures along the bedding direction tends to be inhibited in favor of new shorter bedding-parallel fractures nucleating along the fault plane direction (Fig. 17d).

The mechanical re-compaction of the EDZ in response to packer inflation was simulated by assigning a radial pressure of 3 MPa on the inner model boundary. As shown in Fig. 18a, a zone of high fracture aperture (corresponding to high fracture transmissivity) develops in the microtunnel sidewalls during the preceding EDZ formation process. In response to packer inflation a substantial fracture aperture reduction is simulated around the opening (Fig. 18b), indicating a 64% decay in the total fracture porosity value.

4.6 Hydraulic conductivity around the HG-A microtunnel

Drawing on the workflow described in Fig. 12, the FDEM based discrete fracture networks around the HG-A microtunnel were converted into cell-based distributions of

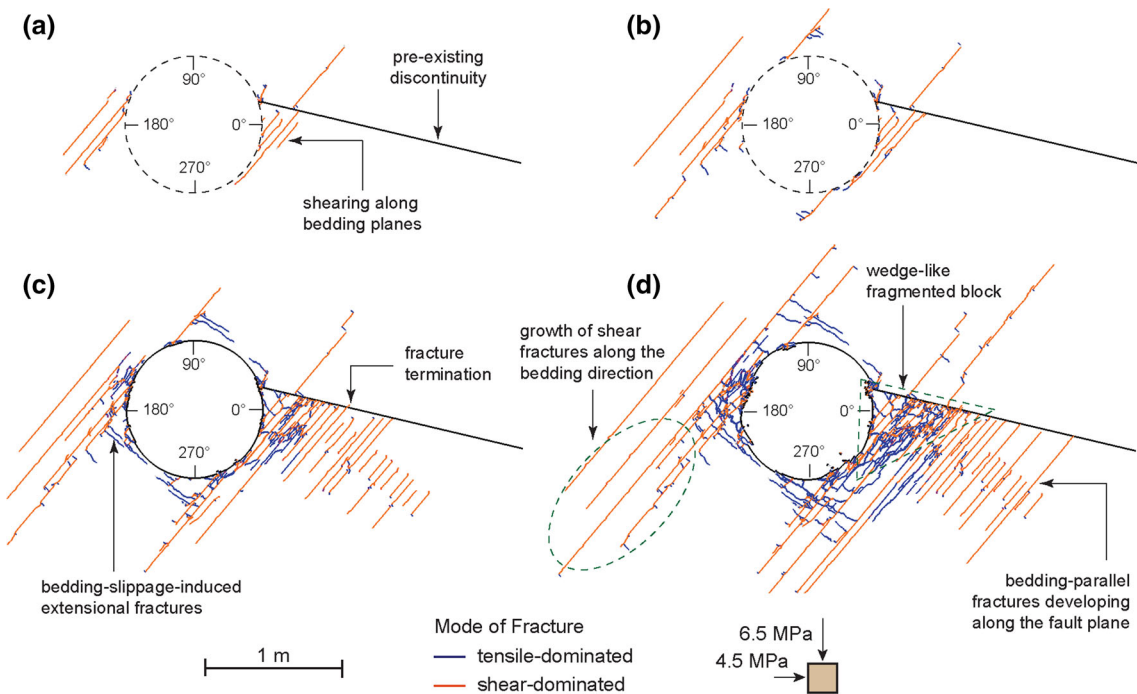
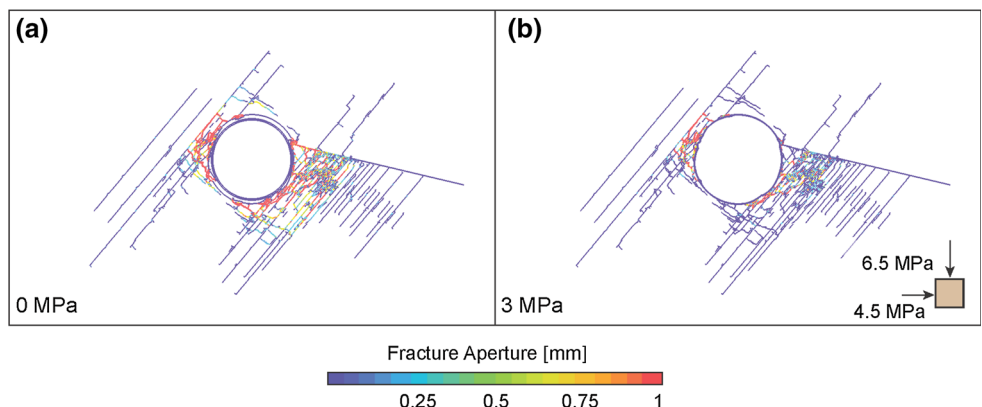


Fig. 17 Simulated EDZ formation process in a model that explicitly accounts for the presence of a sub-horizontal, SW-dipping tectonic fault in the right sidewall [FDEM model “HG-A-F” after Lisjak et al.

(2016)]: **a** 50,000 time steps, **b** 100,000 time steps, **c** 140,000 time steps, and **d** 200,000 time steps

Fig. 18 Spatial distribution of fracture aperture **a** at the time of packer installation and **b** after reaching equilibrium conditions under the effect of a 3 MPa radial pressure, in a model explicitly accounting for the presence of a sub-horizontal, SW-dipping tectonic fault (FDEM model “HG-A-F”; after Lisjak et al. 2015)



effective porosity and hydraulic conductivity (Alcolea et al. 2016). To this end, a finite element mesh was created over which the fracture traces and corresponding fracture characteristics (fracture mode, trace length, aperture) were mapped on the corresponding cells. Effective porosity and effective conductivity values were assigned to each cell by “box-counting” the contributions of the intact rock matrix and traces of the intersecting fractures. A porosity of 12% and a hydraulic conductivity of 4.5×10^{-14} m/s were assigned to the intact rock, representing the properties of the Opalinus Clay at the transition between shaly and sandy

facies. In the conceptual framework, self-sealing of the fractures in response to pore pressure changes (Fig. 13) was mimicked by a swelling mechanism. Thus, the increase of pore pressure from very low negative values (suction) during the unsaturated phase towards static formation pressures in the saturated state after full pore pressure recovery increases the porosity of intact matrix and reduces the aperture of the fracture traces. Based on the available experimental data (Fig. 10), a hyperbolic fracture closure mechanism (Barton-Bandis relationship) was adopted to simulate the reduction of fracture transmissivity in response to pore pressure

increase. Correspondingly, the increase of matrix conductivity associated with the swelling process was expressed in terms of a well-established porosity–permeability relationship (Kozeny–Karman relationship). Further details of the adopted models for simulating the self-sealing of the EDZ are found in Alcolea et al. (2016).

With the given approach, the initial distributions of effective porosity and conductivity around the HG-A microtunnel and their evolution with pore pressure recovery have been calculated for all FDEM fracture network realisations. At early times, when pore pressure in the fracture network is negative due to unsaturated conditions and efficient swelling of the intact matrix does not yet apply, the hydraulic conductance of the EDZ is dominated by the contribution of the highly transmissive fractures, displaying effective conductivities which are many orders of magnitudes higher than the parameters of the intact rock (Fig. 19b). Conversely, when fractures are essentially closed after complete pore pressure recovery, the effective hydraulic conductivity of the EDZ is largely controlled by the matrix behaviour. Figure 18c, d display the late-time distributions of effective porosity and conductivity for the FDEM that

includes the tectonic fracture (Fig. 19a). Cell-based porosities in the immediate vicinity of the microtunnel range between 12 and 40%. Local conductivity values spread between 10^{-11} and 4.5×10^{-14} m/s, which is in general agreement with experimental evidence (see Lanyon et al. 2014).

4.7 Back analysis of water/gas injections: examples

The cell-based distributions of effective porosity and hydraulic conductivity around the HG-A microtunnel, in combination with the implemented self-sealing mechanism (i.e., pressure-controlled fracture closure and swelling of the intact matrix blocks) formed the input for back analyses of the long-term water injections and the gas injection tests.

The multi-rate water injection test described earlier (Fig. 16) was selected for assessing the self-sealing behaviour of the EDZ around the HG-A microtunnel. Pore pressure transients from the piezometer boreholes HG-A2 and HG-A3 (Fig. 14) were used to infer—via maximum likelihood optimization—the fracture closure parameter that controls the closure law (Barton–Bandis like) mimicking the long-term self-sealing of the EDZ. Two different

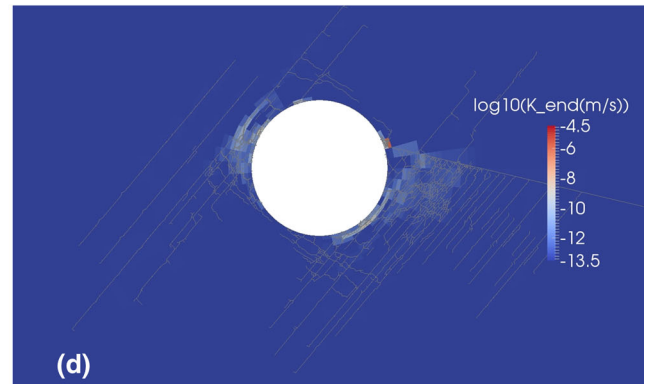
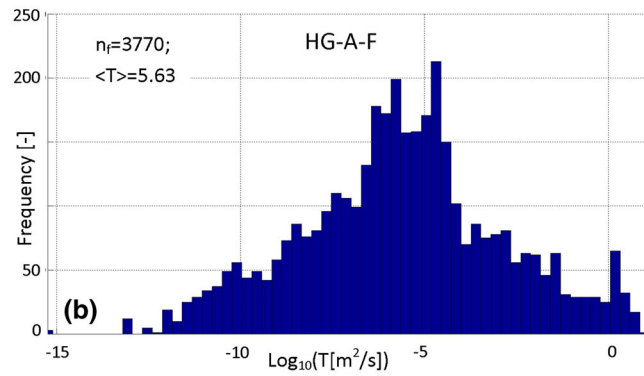
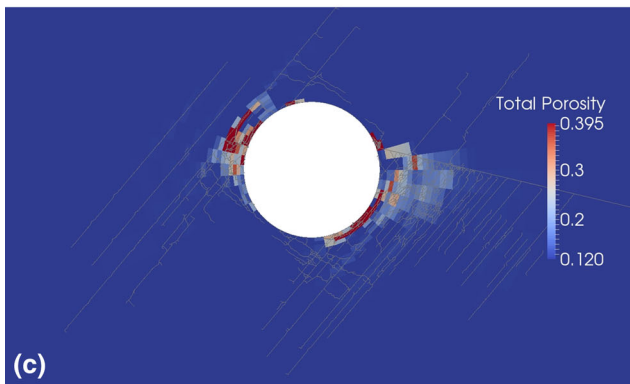
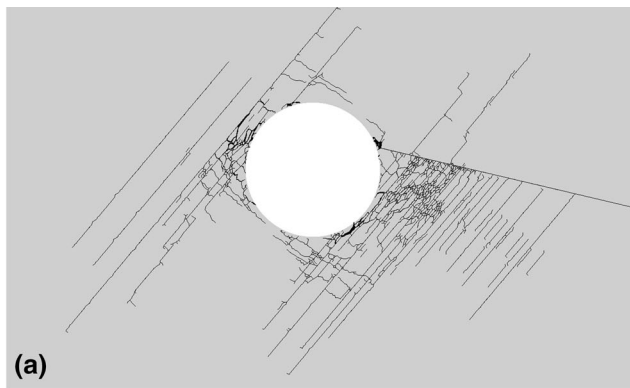


Fig. 19 Modelling of effective EDZ properties around the HG-A microtunnel: **a** FDEM fracture network model with tectonic feature (“HG-A-F”), **b** histograms of initial fracture transmissivity. In the insets, $\langle T \rangle$ denotes the geometric mean of transmissivity, **c**, **d** equivalent porous medium properties on a finite element mesh: late time distributions (after Alcolea et al. 2016)

insets, $\langle T \rangle$ denotes the geometric mean of transmissivity, **c**, **d** equivalent porous medium properties on a finite element mesh: late time distributions (after Alcolea et al. 2016)

FDEM variants of the EDZ fracture network were considered, namely a variant without tectonic faults (FDEM model “HG-A”; see Lisjak et al. 2016) and a variant with a SW-dipping pre-existing discontinuity (Fig. 17; FDEM model “HG-A-F”). Even at early times, model HG-A is characterised by a low hydraulic conductance due to its relatively low fracture density, as compared to model HG-A-F. Figure 20a displays the pressure fits at observation borehole HG-A2 for both models. In spite of the simplistic representation of the model domain (2-D model geometry) and the hydro-mechanical boundary conditions (axisymmetric pressure field and plane stress conditions), the model exhibits relatively good fits of available measurements (see for instance, the time period 300–400 days, Fig. 20a) and captures the main trends of the measured pressure records at the piezometer boreholes in response to the multi-step water injection. Overall, model HG-A-F performs slightly better, suggesting that increased fracture density is more representative for the EDZ around the HG-A microtunnel than the sparse fracture network of the HG-A model.

Gas injection test GI-2 with a gas injection period of 5 months was selected for assessing the gas transport behaviour of the EDZ along the seal section. The simulations were executed with the two-phase flow code TOUGH2 (Pruess et al. 2012) using the FDEM fracture model HG-A-F and the fracture closure parameter determined after the analysis of the long-term water injection test. The simulated gas pressure build-up in the test zone of the HG-A microtunnel and the modelled pressure transients along the seal section are in good agreement with the monitored piezometer data. Clear evidence was seen for a preferential gas flow path, associated with the extended damage zone around the tectonic fault. Figure 20b displays the gas path along the seal section in terms of gas saturation at the time when the gas breakthrough to the Gallery 04 is observed. The modelling results were achieved without extensive calibration of the conductivity and porosity distributions, indicating a good performance of the applied model set-up. Further adaptions of the capillary pressure and relative permeability relationships (cubic scaling law instead of Leverett scaling; Grant gas permeability curve) provided further improvements of the data fits.

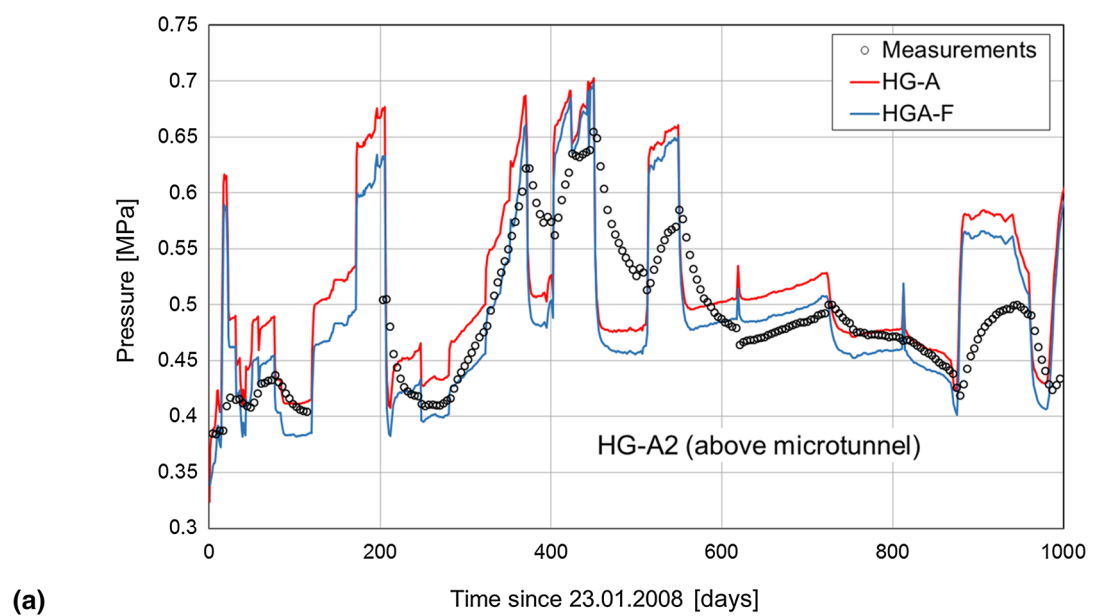
5 Conclusions

In the framework of the Mont Terri Project, new insights have been gained concerning the formation and evolution of the EDZ in indurated clays. Clear evidence was found,

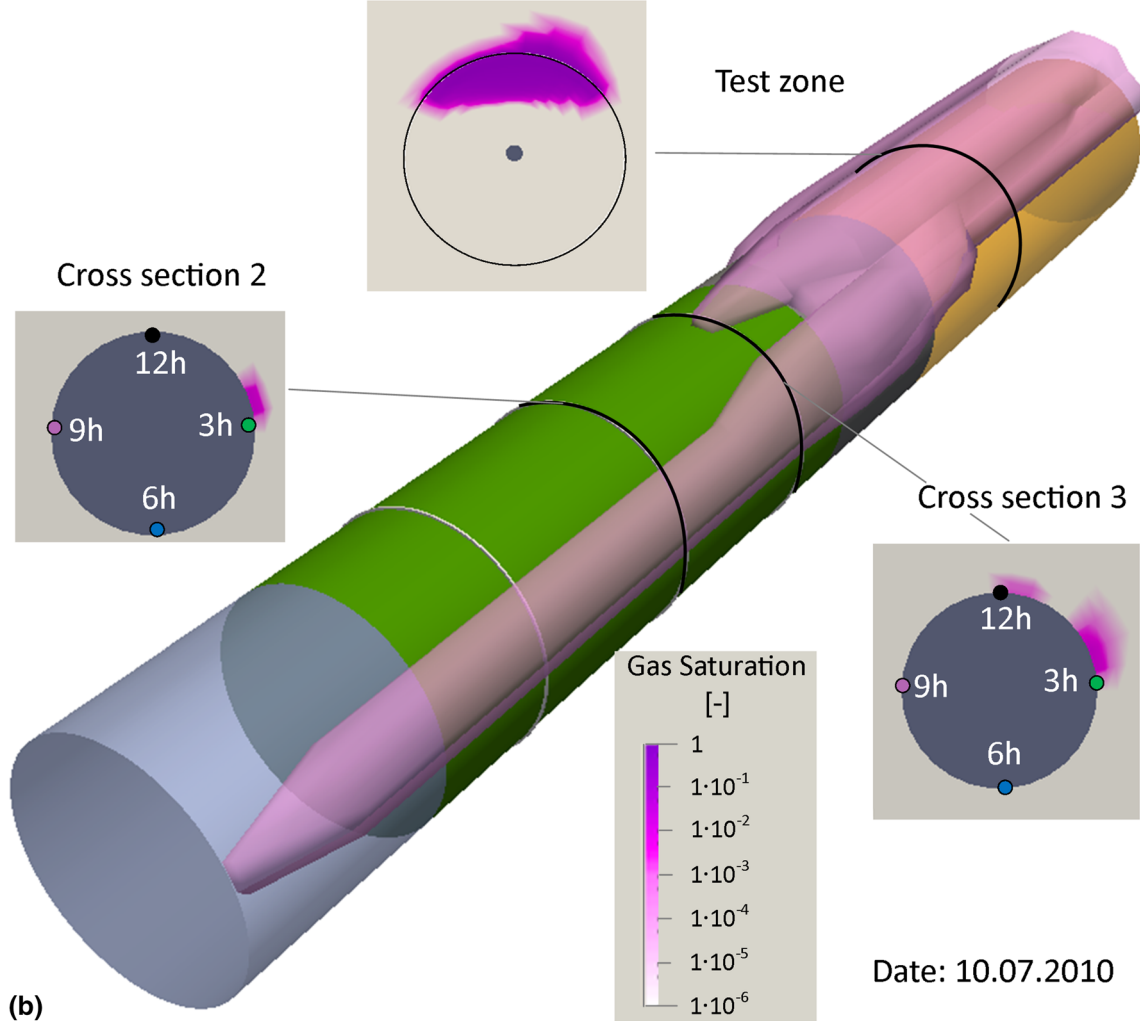
that the immediate (short-term) failure of the Opalinus Clay in response to the excavation process is brittle. The inventory of EDZ-related features comprises extensional fracturing, bedding parallel slip, buckling and kink failures, isolated shear fractures, shear bands and reactivated tectonic features. Multiple examples of stress controlled failure have been reported, all suggesting that the *in situ* virgin stress and the stress state ahead of the tunnel face govern the formation of the EDZ. As a consequence, the extent of stress controlled failure is strongly influenced by the choice of excavation technique and the progress of excavation. On the other hand, structurally controlled failure is related to the occurrence of sedimentary and tectonic structures. Variabilities in microstructure such as bedding or intercalations of sandy and clay-rich layers tend to create self-similar failure patterns (e.g. buckling), which are observed at scales ranging from small boreholes to the tunnel scale. In contrast, reactivations of tectonic structures are highly irregular processes and are therefore difficult to predict without detailed knowledge of the pre-existing fracture patterns, a fact which calls for detailed site characterisation measures ahead of the excavation face.

A mechanistic understanding of the hydro-mechanical and hydro-chemical phenomena associated with the self-sealing capacity of the Opalinus Clay has been developed. In this context, a long-lasting packer test campaign in short radial boreholes allowed to bracket the time scales and magnitudes of EDZ fracture self-sealing, indicating a continuous decrease of fracture transmissivities by several orders of magnitudes within a time period of three years. Furthermore, a dedicated *in situ* experiment on a hydraulic fracture revealed the hydro-mechanical controls, essentially determining the hydraulic significance of the EDZ fractures. In this context, a hyperbolic fracture closure law was derived, expressing for a functional relationship between fracture transmissivity and the prevailing pore pressure (respectively, effective normal stress) when the fracture is subjected to a normal (total) stress component.

The comprehensive experimental data base of the Mont Terri research programme formed the basis for the development of a versatile heuristic modelling approach, aimed at simulating flow and transport processes along the EDZ and capable to estimate the spatial-temporal evolution of hydraulic conductance of the EDZ after tunnel closure. The model was benchmarked with a data set from the HG-A experiment, demonstrating the ability of the approach to mimic the evolution of the hydraulic conductance of the EDZ around a backfilled tunnel section during the entire re-saturation phase. In addition, a two-phase flow model was successfully applied for the back-analysis of gas injection



(a)



(b)

◀ Fig. 20 Back analysis of a long-term water injection and a gas injection test at the HG-A experiment (from Alcolea and Kuhlmann 2017): **a** simulation of a long-term water injection test with the fracture network models “HG-A” and “HG-A-F”. The pressure fits at observation borehole HG-A2 above the tunnel are displayed; **b** simulation of gas injection test GI-2 with the fracture network model HG-A-F. The preferential gas path along the EDZ at the time of the gas breakthrough is indicated by enhanced gas pressures

tests, giving evidence for the high gas transport capacity of the EDZ along a sealed tunnel section. The suggested methodology provides an abstracted single-shell model of the EDZ, able to mimic the relevant functional features of the EDZ in a traceable manner. Such abstracted model is a requirement for radionuclide release calculations in support of long-term safety analyses of a geological repository.

Acknowledgements This work was supported by ANDRA, BGR, Nagra and NWMO via the Mont Terri Consortium. The authors would like to thank Dr. Paul Bossart, Mr. T. Theurillat, Dr. D. Jäggi of the Mont Terri consortium together with the many contractors who have supported the experiments for their invaluable assistance in the technical planning and performance of the experiment. The valuable review comments and suggestions by Prof. D. Martin (University of Edmonton, Canada) and Prof. T.S. Nguyen (Canadian Nuclear Safety Commission, Ottawa) for improving the technical quality of this paper are highly appreciated.

References

- Alcolea, A., Kuhlmann, U. (2017). Mont Terri HG-A experiment (phase 21). Inverse few modelling of the hydraulic properties of the EDZ. Mont Terri Technical Note 2016-76 (*in prep.*)
- Alcolea, A., Kuhlmann, U., Marschall, P., Lisjak, A., Grasselli, G., Mahabadi, O., de La Vaissière, R., Leung, H., & Shao, H. (2016). A pragmatic approach to abstract the EDZ around tunnels of a geological radioactive waste repository—Application to the HG-A experiment in Mont Terri. *Geological Society, London, Special Publications*, 443, SP443-8.
- Alcoverro, J., Olivella, S., & Alonso, E. E. (2014). Modelling fluid flow in Opalinus Clay excavation damage zone. A semi-analytical approach. *Geological Society, London, Special Publications*, 415(1), 143–166.
- Alheid, H. J., Aranyossy J. F., Blümling P., Hoteit N., & Van Geet M. (2007). EDZ Development and Evolution (RTDC 4). EDZ development and evolution. State of the art. *NF-PRO. Contract Number F16W-CT-2003-02389*. European Commission, Luxembourg.
- Aranyossy, J. F., Mayor, J. C., Marschall, P., Plas, F., Blumling, P., Van Geet, M., Armand, G., Techer, I., Alheid, A. J., Rejeb, A., Pinettes, P., Balland, C., Popp, T., Rothfuchs, T., Matray, J. M., De Craen, M., Wieczorek, K., Pudewills, A., Czaikowski, O., Hou, Z., & Fröhlich, H. (2008). EDZ Development and Evolution (RTDC 4). In *nuclear science and technology. Understanding and Physical and Numerical Modelling of the Key Processes in the Near Field and their Coupling for Different Host Rocks and Repository Strategies NF-PRO) Final Synthesis Report (D. 4.5.3)*. FP6-EURATOM/NF-PRO, F16W-CT-2003-02389 (pp. 150–197). European Commission, Luxembourg.
- Armand, G., Leveau, F., Nussbaum, C., De La Vaissière, R., Noiret, A., Jaeggi, D., et al. (2013a). Geometry and properties of the excavation-induced fractures at the Meuse/Haute-Marne URL drifts. *Rock Mechanics and Rock Engineering*, 47(1), 21–41.
- Armand, G., Noiret, A., Zghondi, J., & Seyed, D. M. (2013b). Short- and long-term behaviors of drifts in the Callovo-Oxfordian claystone at the Meuse/Haute-Marne underground research laboratory. *Journal of Rock Mechanics and Geotechnical Engineering*, 5(3), 221–230.
- Blümling, P., Bernier, F., Lebon, P., & Martin, C. D. (2007). The excavation damaged zone in clay formations time-dependent behaviour and influence on performance assessment. *Physics and Chemistry of the Earth, Parts A/B/C*, 32(8), 588–599.
- Bossart, P., Bernier, F., Birkholzer, J., Bruggeman, C., Connolly, P., Dewonck, S., Fukaya, M., Herfort, M., Jensen, M., Matray, J.-M., Mayor, J. C., Moeri, A., Oyama, T., Schuster, K., Shigeta, N., Vietor, T., & Wieczorek, K. (2017). Mont Terri rock laboratory, 20 years of research: introduction, site characteristics and overview of experiments. *Swiss Journal of Geosciences*, 110. doi:10.1007/s00015-016-0236-1 (this issue).
- Bossart, P., Meier, P. M., Moeri, A., Trick, T., & Mayor, J. C. (2002). Geological and hydraulic Characterization of the excavation disturbed zone in the Opalinus Clay of the Mont Terri Rock Laboratory. *Engineering Geology*, 66, 19–38.
- Bossart, P., Trick, T., Meierand, P. M., & Mayor, J. C. (2004). Structural and hydrogeological Characterization of the excavation-disturbed zone in the Opalinus Clay (Mont Terri Project, Switzerland). *Applied Clay Science*, 26, 429–448.
- Diederichs, M. S., & Kaiser, P. K. (1999). Stability of large excavations in laminated hard rock masses: the Voussoir analogue revisited. *International Journal of Rock Mechanics and Mining Sciences*, 36(1), 97–118.
- DIT-UPC. (2000). *CODE_BRIGHT, A 3-D program for thermo-hydro-mechanical analysis in geological media. User's guide*. Barcelona: CIMNE.
- Einstein, H. H. (2002). Tunnels in Opalinus Clayshale. A review of case histories and new developments. *Tunnelling and Underground Space Technology*, 15(1), 13–29.
- Ferrari, A., Favero, V., Marschall, P., & Laloui, L. (2014). Experimental analysis of the water retention behaviour of shales. *International Journal of Rock Mechanics and Mining Sciences*, 72, 61–70.
- Harrington, J., Volckaert, G., Jacobs, E., Maes, N., Areias, L., Charlier, R., & Granet, S. (2013). Summary report: experiments and modelling of excavation damage zone (EDZ) behaviour in argillaceous and crystalline rocks (Work Package 4). *EC FORGE Project Report D*, 4.
- Itasca. (2012). *FLAC3D (Fast Lagrangian Analysis of Continua). Version 5.01*. Itasca Consulting Group Inc., Minnesota, USA.
- Labiouse, V., & Vietor, T. (2014). Laboratory and in situ simulation tests of the excavation damaged zone around galleries in Opalinus Clay. *Rock Mechanics and Rock Engineering*, 47(1), 57–70.
- Lanyon, G. W. (2011). Excavation damaged zones assessment. *Report NWMO DGR-TR-25 2011-21*. (p. 111).
- Lanyon, G. W., Marschall, P., Trick, T., De La Vaissiere, R., Shao, H., & Leung, H. (2009). Hydromechanical Evolution and Self-Sealing of Damage Zones around a Microtunnel in a Claystone Formation of the Swiss Jura Mountains. In *43rd U.S. Rock Mechanics Symposium & 4th U.S.—Canada Rock Mechanics Symposium* (pp. 652–663). American Rock Mechanics Association.
- Lanyon, G. W., Marschall, P., Trick, T., De La Vaissiere, R., Shao, H., & Leung, H. (2014). Self-sealing experiments and gas injection tests in a backfilled microtunnel of the Mont Terri URL. *Geological Society, London, Special Publications*, 400(1), 93–106.
- Lanyon, G. W., & Senger, R. (2011). A Structured approach to the derivation of effective properties for combined water and gas flow in the EDZ. *Transport in Porous Media*, 90(1), 95–112.

- Lisjak, A., Garitte, B., Grasselli, G., Müller, H., & Vietor, T. (2015). The excavation of a circular tunnel in a bedded argillaceous rock (Opalinus Clay): short-term rock mass response and FDEM numerical analysis. *Tunnelling and Underground Space Technology*, 45, 227–248.
- Lisjak, A., Tatone, B. S. A., Mahabadi, O. K., Grasselli, G., Marschall, P., Lanyon, G. W., et al. (2016). Hybrid finite-discrete element simulation of the EDZ formation and mechanical sealing process around a microtunnel in Opalinus Clay. *Rock Mechanics and Rock Engineering*, 49(5), 1849–1873.
- Marschall, P., Distinguin, M., Shao, H., Bossart, P., Enachescu, C., & Trick, T. (2006). Creation and evolution of damage zones around a microtunnel in a claystone formation of the Swiss Jura Mountains. In *International Symposium and Exhibition on Formation Damage Control*, Society of Petroleum Engineers.
- Marschall, P., Horseman, S., & Gimmi, T. (2005). Characterisation of gas transport properties of the Opalinus Clay, a potential host rock formation for radioactive waste disposal. *Oil & Gas Science and Technology*, 60(1), 121–139.
- Marschall, P., Trick, T., Lanyon, G. W., Delay, J., & Shao, H. (2008). Hydro-Mechanical Evolution of Damaged Zones around a Microtunnel in a Claystone Formation of the Swiss Jura Mountains. In *The 42nd US Rock Mechanics Symposium (USRMS)*, American Rock Mechanics Association.
- Martin, C. D., Christiansson, R., & Söderhäll, J. (2001). Rock stability considerations for siting and constructing a KBS-3 repository. *SKB Technical Report*, TR-01-38 (p. 94). Swedish Nuclear Fuel and Waste Management Co, Stockholm, Sweden. <http://www.skb.se>.
- Martin, C. D., & Lanyon, G. W. (2003). EDZ in clay shale: Mont Terri. *Mont Terri Technical Report*, TR 01-01 (p. 207). Federal Office of Topography (swisstopo), Wabern, Switzerland. <http://www.mont-terri.ch>.
- Nagra. (1997). Geosynthese Wellenberg 1996-Ergebnisse der Untersuchungsphasen I und II. *Nagra Technical Report*, NTB 96-01 (p. 511). Nagra, Wettingen, Switzerland. <http://www.nagra.ch>.
- Nagra. (2002). Projekt Opalinuston. Synthese der geowissenschaftlichen Untersuchungs ergebnisse. Entsorgungsnachweise für abgebrannte Brennelemente, verglaste hochaktive sowie langlebige mittelaktive Abfälle. *Nagra Technical Report*, NTB 02-03 (p. 659). Nagra, Wettingen, Switzerland. <http://www.nagra.ch>.
- Nagra. (2008). Effects of post-disposal gas generation in a repository for low- and intermediate-level waste sited in the Opalinus Clay of Northern Switzerland. *Nagra Technical Report*, NTB 08-07 (p. 175). Nagra, Wettingen, Switzerland. <http://www.nagra.ch>.
- Nagra. (2016). Production, consumption and transport of gases in deep geological repositories according to the Swiss disposal concept. *Nagra Technical Report*, NTB 16-03, Nagra, Wettingen, Switzerland. <http://www.nagra.ch>.
- Nguyen, T. S., & Le, A. D. (2015). Simultaneous gas and water flow in a damage-susceptible bedded argillaceous rock. *Canadian Geotechnical Journal*, 52(1), 18–32.
- Nussbaum, C., Kloppenburg, A., Caér, T., & Bossart, P. (2017). Tectonic evolution around the Mont Terri rock laboratory, northwestern Swiss Jura: constraints from kinematic forward modelling. *Swiss Journal of Geosciences*, 110. doi:[10.1007/s00015-016-0248-x](https://doi.org/10.1007/s00015-016-0248-x) (this issue).
- Poller, A., Smith, P., Mayer, G., & Hayek, M. (2014). Modelling of Radionuclide Transport along the Underground Access Structures of Deep Geological Repositories. *Nagra Technical Report*, NTB 14-10 (p. 166). Nagra, Wettingen, Switzerland. <http://www.nagra.ch>.
- Pruess, K., Oldenburg, C., & Moridis, G. (2012). TOUGH2 user's guide, Version 2.1 Lawrence Berkeley Laboratories, *Report LBL-43134*, Berkeley, CA, USA.
- Rejeb, A., Slimane, K. B., Cabrera, J., Matray, J. M., & Savoye, S. (2008). Hydro-mechanical response of the Tournemire argillite to the excavation of underground openings: Unsaturated zones and mine-by-test experiment. In *Thermo-hydromechanical and chemical coupling in geomaterials and applications: proceedings of the 3 international symposium GeoProc'2008* (pp. 649–656). Wiley.
- Senger, R. K., Lanyon, G. W., & Marschall, P. (2013). Modeling the Hydraulic and Two-phase Flow Behaviour of the Heterogeneous, Fractured EDZ in the Opalinus Clay during the HG-A Experiment at the Mont Terri URL. In *Proceedings of the Fourth European Association of Geoscientists & Engineers (EAGE) Shale workshop. Shales: what do they have in common?* (pp 148–152). European Association of Geoscientists & Engineers.
- Shao, H., Xu, W., Marschall, P., Kolditz, O., & Hesser, J. (2015). Numerical interpretation of gas-injection tests at different scales. *Geological Society, London, Special Publications*, 415(1), 203–212.
- Steiner, W. (1996). Tunnelling in squeezing rocks: case histories. *Rock Mechanics and Rock Engineering*, 29(4), 211–246.
- Suckling, P., Avis, J., Calder, N., Humphreys, P., King, F., & Walsh, R. (2012). T2GGM Version 3.1: gas generation and transport code. *Nuclear Waste Management Organization Report NWMO TR-2012-23*. Toronto, Canada.
- Tsang, C. F., Bernier, F., & Davies, C. (2005). Geohydromechanical processes in the Excavation Damaged Zone in crystalline rock, rock salt, and indurated and plastic clays in the context of radioactive waste disposal. *International Journal of Rock Mechanics and Mining Sciences*, 42(1), 109–125.
- Walsh, R., Nasir, O., Leung, H., & Avis, J. (2015). Numerical Characterization of the Excavation Damaged Zone in the HG-A Experiment. In *Proceedings: International High-Level Radioactive Waste Management*, Charleston, SC.
- Wilson, C. R., Witherspoon, P. A., Long, J. C. S., Galbraith, R. M., DuBois, A. O., & McPherson, M. J. (1983). Large-scale hydraulic conductivity measurements in fractured granite. *International Journal of Rock Mechanics and Mining Sciences & Geomechanics Abstracts*, 20(6), 269–276.
- Xu, W., Shao, H., Marschall, P., Hesser, J., & Kolditz, O. (2013). Analysis of flow path around the sealing section HG-A experiment in the Mont Terri Rock Laboratory. *Environmental Earth Sciences*, 70(7), 3363–3380.
- Yong, S. (2007). A three-dimensional analysis of excavation-induced perturbations in the Opalinus Clay at the Mont Terri Rock Laboratory. *Ph.D dissertation*, Swiss Federal Institute of Technology in Zürich, Zürich, Switzerland, p. 167.